

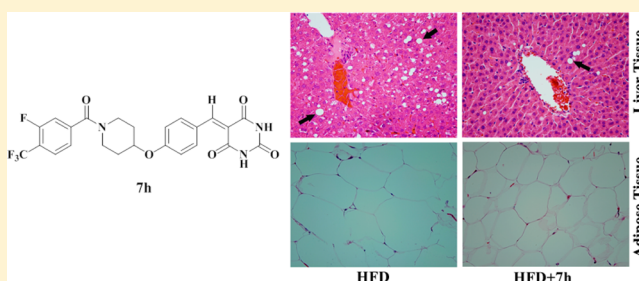
Synthesis and Biological Evaluation of 5-Benzylidenepyrimidine-2,4,6(1*H*,3*H*,5*H*)-trione Derivatives for the Treatment of Obesity-Related Nonalcoholic Fatty Liver Disease

Liang Ma, Caifeng Xie, Yan Ran, Xiaolin Liang, Li Huang, Heying Pei, Jinying Chen, Juan Liu, Yun Sang, Huijun Lai, Aihua Peng, Mingli Xiang, Yuquan Wei, and Lijuan Chen*

State Key Laboratory of Biotherapy, West China Hospital, West China Medical School, Sichuan University, Keyuan Road 4, Gaopeng Street, Chengdu 610041, China

Supporting Information

ABSTRACT: Nonalcoholic fatty liver disease (NAFLD), one of chronic liver diseases, seems to be rising as the obesity epidemic continues. In this study, 54 novel (thio)barbituric acid derivatives have been synthesized and evaluated for pharmacological activity. **7h** exhibited potent glucose-lowering effects on insulin-resistant HepG2 cells and regulated adiponectin and leptin expression in 3T3-L1 adipocytes. Oral administration of **7h** at 25 mg kg⁻¹ day⁻¹ for 4 weeks improved the progression of high fat diet-induced NAFLD by reducing the weight of body, liver, and fat, as well as modulating serum levels of fasting glucose, insulin, triglycerides, LDL-c, ALT, adiponectin and hepatic contents of triglycerides, total cholesterol. H&E stainings revealed that **7h** blocked fat deposition in liver and the increase of adipocyte number and size in adipose tissues from NAFLD. Furthermore, treatment with **7h** alleviated the obese clinical symptoms, recovered serum biomarkers to appropriate ranges, and improved glucose tolerance by OGTT and IGTT in DIO mice.



INTRODUCTION

Nonalcoholic fatty liver disease (NAFLD), one of the leading causes of chronic liver diseases, affects approximately 20–30% of the general population in Western countries, and the incidence seems to be rising as the obesity epidemic continues.^{1–3} NAFLD, defined by fat infiltration and accumulation exceeding 5–10% per liver weight, is a clinicopathological hepatic steatosis without a history of excess alcohol consumption.⁴ The histological spectrum of the disease comprises primary fatty liver, nonalcoholic steatohepatitis (NASH), and NAFLD-associated fibrosis, cirrhosis, and hepatocellular carcinoma (HCC).⁵ The advanced forms of NAFLD are more common in obese patients who exhibit several features of metabolic syndrome—central obesity, type 2 diabetes, dyslipidemia, and atherosclerosis, arising from insulin resistance and abnormal levels of adipokines.^{6,7} As yet, there is no convincingly effective treatment for NAFLD, but a multimodal therapeutic plan that targets obesity, insulin resistance, and adipokines might be the optimal choice for these patients.⁸

A series of adipokines, such as adiponectin and leptin, play key roles in modulating insulin-related glucose homeostasis and lipid metabolism in adipose tissues of obese NAFLD patients.^{9,10} Adiponectin, a 247-amino acid collagen-like polypeptide, is the most abundant and adipose-specific adipokine.¹¹ The level of adiponectin is correlated negatively with insulin, blood glucose, triglycerides, and LDL-c but

correlated positively with HDL-c.^{12–14} Adiponectin possesses a hepatoprotective effect, as it increases the viability of liver cells and insulin sensitivity, and attenuates the lipid inflation in liver of NAFLD.² Similarly, leptin, the product of the obese gene, is an adipocyte-secreted protein hormone with a key role in food intake, energy expenditure, and glucose homeostasis.^{10,15} Therefore, the functions of adiponectin and leptin in adipocytes or adipose tissues for regulating insulin as well as glucose and fat metabolism make them potential therapeutic targets for NAFLD.

Although the pathogenesis of NAFLD is not fully elucidated, insulin resistance is a common occurrence in obese NAFLD patients and characterized by reducing insulin sensitivity. Insulin increases glucose uptake in fat and muscle and inhibits the output and release of hepatic glucose, thus serving as the primary modulator of blood glucose level. Insulin also promotes the storage of substrates in liver and fat tissues by stimulating lipogenesis and inhibiting lipolysis.¹⁶ Insulin resistance or deficiency results in profound dysregulation of these processes and further interferes with the metabolism of glucose and lipid. Lifestyle modifications with diet and exercise could improve insulin sensitivity and are the cornerstone of therapy but are often difficult to maintain long-term. Not surprisingly, considerable studies have been focused on

Received: August 7, 2012

Published: October 1, 2012

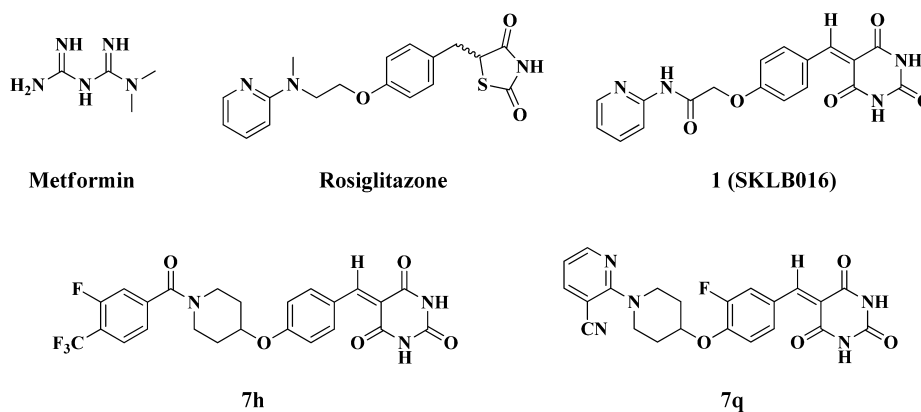
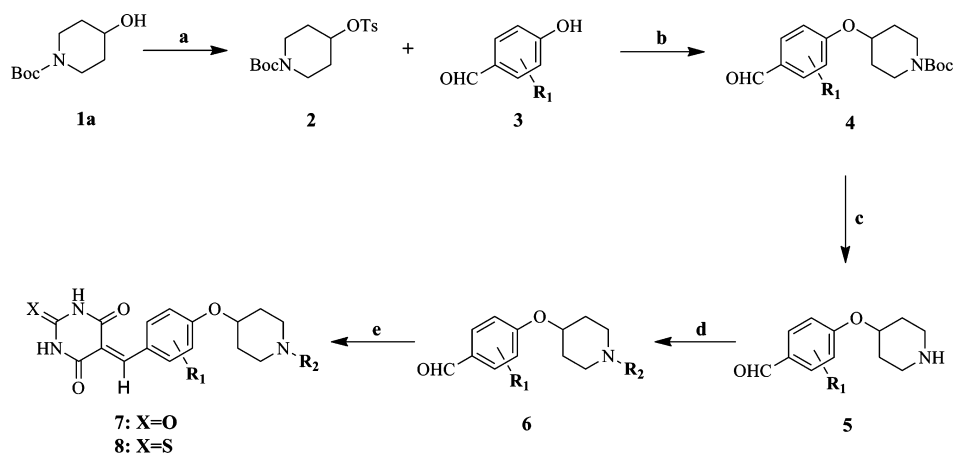


Figure 1. Chemical structure of metformin, rosiglitazone, 1, 7h, and 7q.

Scheme 1. Synthesis of 7 and 8^a



^aReagents and conditions: (a) TsCl, pyridine, 0 °C to room temperature, overnight; (b) K₂CO₃, DMF, 100 °C, 8 h; (c) TFA, CH₂Cl₂, 4 h. (d) Procedure A: R₂COOH, EDCI, DMAP, CH₂Cl₂, room temperature, overnight. Procedure B: R₂Cl, K₂CO₃, DMF, 100 °C. (e) (Thio)barbituric acid, ethanol, water, 60 °C, 3–4 h.

exploring and developing potent and novel insulin regulators as therapeutic potential for the treatment of obesity-related NAFLD.

In our recent publication, we described our research efforts that began with an adiponectin and leptin screening from our libraries of (thio)barbituric acid derivatives^{17,18} and thiazolidinediones (TZDs),¹⁹ which culminated in the identification of 5-benzylidenepyrimidine-2,4,6(1*H*,3*H*,5*H*)-trione derivative 1 (SKLB016, Figure 1) as a potent drug lead for the treatment of NAFLD by regulating blood glucose level and adipokine expressions to improve insulin resistance. With the objective of developing therapeutic agents for obesity-related NAFLD with optimal biopharmaceutical properties, the structural modifications on the basis of 1 led to two novel and potent agents against the animal model of obesity-related NAFLD, which were designated as barbituric acid derivatives 7h and 7q (Figure 1).

CHEMISTRY

The preparation of a library of 5-benzylidenepyrimidine-2,4,6(1*H*,3*H*,5*H*)-trione and 5-benzylidene-2-thioxodihydropyrimidine-4,6(1*H*,5*H*)-dione derivatives (7 and 8) has been carried out in a tandem five-step sequence from commercially available *tert*-butyl 4-hydroxypiperidine-1-carboxylate (1a) as described in Scheme 1. Treatment of 1a with *p*-toluenesulfonyl

chloride (TsCl) at 0 °C in the solvent of pyridine afforded 2 in a good yield. The pivotal aldehyde intermediates 4 were synthesized via a reaction of 2 and appropriate *p*-hydroxybenzaldehyde in dimethyl formamide (DMF) using anhydrous potassium carbonate (K₂CO₃) as a base. After the deprotection in a solution of TFA/CH₂Cl₂ (v/v, 1/1) in an ice bath, the 5 compounds were treated with corresponding benzoic acids followed by 1-(3-dimethylaminopropyl)-3-ethylcarbodiimide hydrochloride (EDCI) as an efficient condensing agent (procedure A) or appropriate 2-chloropyridines in the presence of anhydrous K₂CO₃ as a base (procedure B) to give the *N*-substituted 6. Finally, the Knoevenagel reaction of 6 with barbituric acid or thiobarbituric acid in a mixture of ethanol and water as valid solvent was heated at 60 °C for 3–4 h to afford the targeted compounds 7 (X = O) and 8 (X = S), summarized in Table 1.

Next, to explore the study of structure–activity relationship (SAR), these novel barbituric acid derivatives 12 were synthesized as outlined in Scheme 2. Compounds 9 were prepared according to the same synthetic procedures reported for 6 starting from commercially available *tert*-butyl piperidin-4-ylcarbamate. After the deprotection of 9 in TFA/CH₂Cl₂ solution, the intermediate salts were basified by stirring in a mixture of K₂CO₃ for 1 h and then reacted with 4-(diethoxymethyl)benzaldehyde at 80 °C overnight and further

Table 1. Structural Information of 7 and 8 for Pharmacological Profiling

No.	R ₁	R ₂	No.	R ₁	R ₂	No.	R ₁	R ₂
7a	3-H		7l	3-H		7w	3-F	
7b	3-H		7m	3-H		7x	3-F	
7c	3-H		7n	3-H		7y	3-F	
7d	3-H		7o	3-F		7z	3-F	
7e	3-H		7p	3-F		8a	3-H	
7f	3-H		7q	3-F		8b	3-H	
7g	3-H		7r	3-F		8c	3-H	
7h	3-H		7s	3-F		8d	3-H	
7i	3-H		7t	3-F		8e	3-OEt	
7j	3-H		7u	3-F		8f	3-OEt	
7k	3-H		7v	3-F		8g	3,4-diOMe	

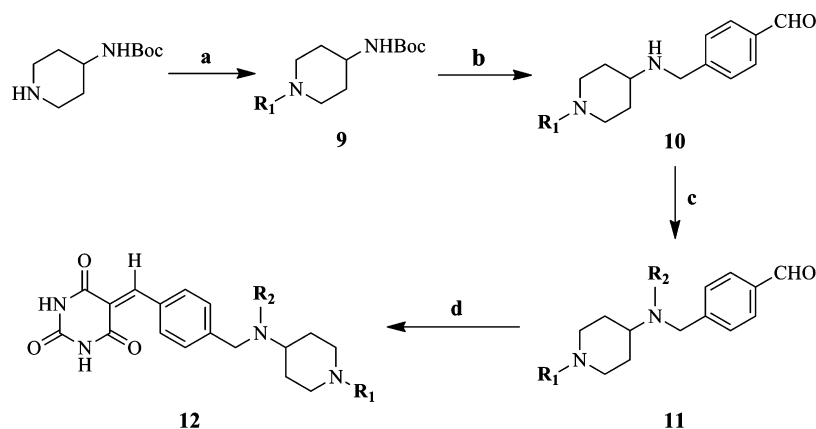
were reduced using sodium borohydride (NaBH₄) in anhydrous methanol to give **10** in a good yield. The condensation of **10** with different aryl(sulfonyl) chlorides followed by triethylamine (Et₃N) as a base (procedure C) or iso(thio)cyanates and butyric anhydride in the presence of pyridine solvent (procedure D) afforded the corresponding aldehydes **11**. The desired derivatives **12** were also obtained by the condensation of **11** with barbituric acid in a solvent of ethanol/water overnight at 60 °C, and their structural information of **12** is summarized in Table 2.

Similarly, **14a–c** (Scheme 3) and **17a,b** (Scheme 4) have been obtained by the condensation of aldehydes with barbituric acid according to the previous procedures in moderate overall yields and in relatively few synthetic steps. The advantages of the Knoevenagel reaction were numerous in this study: all starting aldehydes and (thio)barbituric acid were soluble in hot

water/ethanol; the reaction was clean and quick; the insoluble final compound was precipitated with a purity of more than 95%.²⁰ At this stage, all final products were fully analyzed and characterized by NMR, MS, and HPLC before being submitted to the biological screening.

RESULTS AND DISCUSSION

Liver tissue plays an important role in glucose and fat metabolism. The HepG2 cell (hepatocellular carcinoma cell) is similar to human hepatocyte and is used to evaluate whether **54** novel (thio)barbituric acid derivatives are capable of regulating glucose consumption (GC) in insulin-resistant HepG2 cells.²¹ Simultaneously, the MTT (3-(4,5-dimethylthiazol-2-yl)-2,5-diphenyltetrazolium bromide) assay was performed to investigate whether the glucose-lowering effects are not due to the cytotoxicity of compounds.²² Insulin sensitizers

Scheme 2. Synthesis of 12^a

^aReagents and conditions. (a) Procedure A: R₁COOH, EDCI, DMAP, CH₂Cl₂, room temperature, overnight. Procedure B: R₁Cl, K₂CO₃, DMF, 70 °C. (b) (i) TFA, CH₂Cl₂, 0 °C to room temperature, 3 h; (ii) 4-(diethoxymethyl)benzaldehyde, K₂CO₃, water, EtOH, 80 °C, overnight; (iii) NaBH₄, methanol, 60 °C, 0.5 h; (iv) 1 N HCl, acetone, 0.5 h. (c) Procedure C: R₂COCl or R₂SO₂Cl, Et₃N, CH₂Cl₂, room temperature, overnight. Procedure D: (R₂CO)₂O or iso(thio)cyanate, pyridine, room temperature, overnight. (d) Barbituric acid, ethanol, water, 60 °C, overnight.

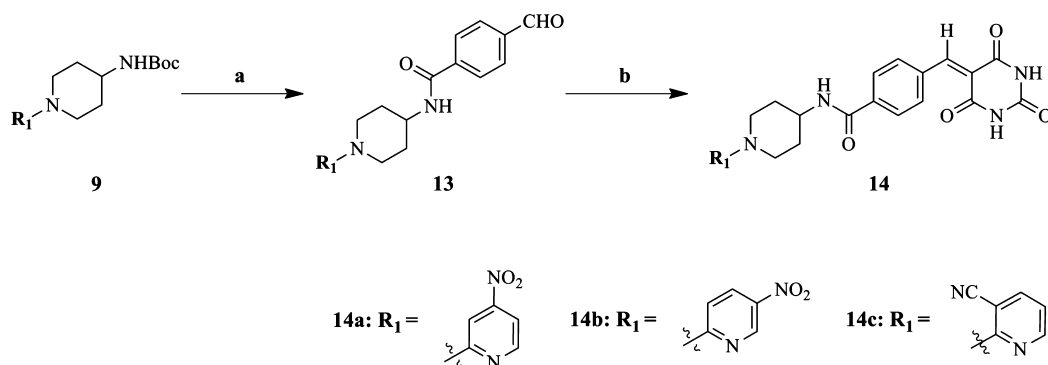
Table 2. Structural Information of 12 for Pharmacological Profiling

No.	R ₁	R ₂	No.	R ₁	R ₂
12a		H	12i		
12b			12j		
12c			12k		
12d		H	12l		
12e			12m		
12f			12n		
12g			12o		
12h			12p		

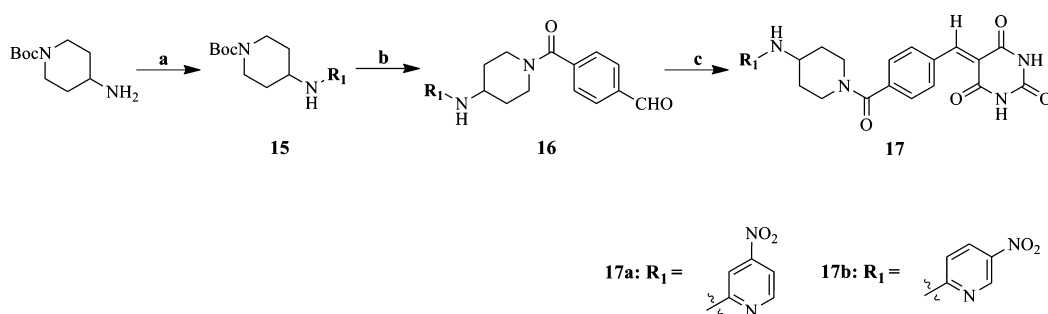
(metformin and rosiglitazone) were selected as positive controls in this study.

As illustrated in Figure 2, the initial screening data from GC/MTT assay indicated that seven compounds (7c, 7g, 7h, 7m, 7q, 7w, and 14b) at 10 μM exhibited more comparable or potent glucose-lowering effects on insulin-resistant HepG2 cells

in the presence of insulin (0.1 μM) and high-glucose condition (22.2 mM glucose) than two marketed drug rosiglitazone and metformin. However, the other derivatives did not effectively promote the process of GC/MTT in contrast to positive control, regardless of the presence of insulin or not, and the additional results are presented in Supporting Information

Scheme 3. Synthesis of 14^a

^aReagents and conditions: (a) (i) TFA, CH₂Cl₂, 0 °C to room temperature, 3 h. (ii) Procedure A: 4-formylbenzoic acid, EDCl, DMAP, CH₂Cl₂, room temperature, overnight. (b) Barbituric acid, ethanol, water, 60 °C, overnight.

Scheme 4. Synthesis of 17^a

^aReagents and conditions. (a) Procedure B: R₁Cl, K₂CO₃, DMF, 70 °C. (b) (i) TFA, CH₂Cl₂, 0 °C to room temperature, 3 h. (ii) Procedure A: 4-formylbenzoic acid, EDCl, DMAP, CH₂Cl₂, room temperature, overnight. (c) Barbituric acid, ethanol, water, 60 °C, overnight.

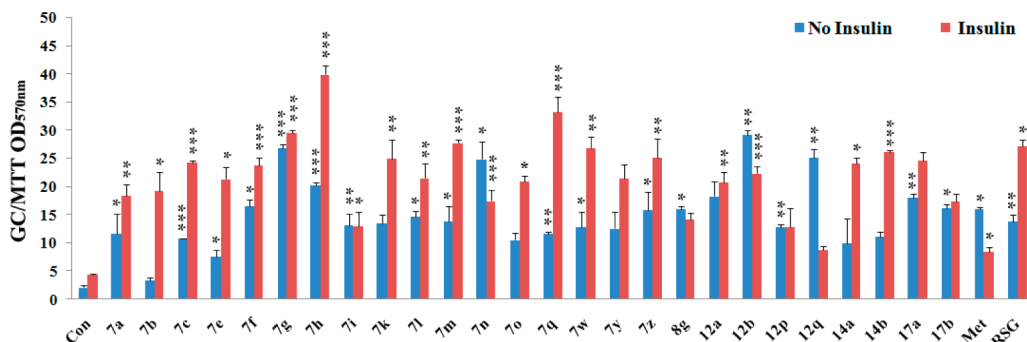


Figure 2. Effects on GC/MTT in insulin-resistant HepG2 cells. 1.0 mM metformin (Met), 10 μ M rosiglitazone (RSG), and compounds 7a–z, 8a–g, 12a–p, 14a–c, and 17a,b at 10 μ M were tested in the DMEM (22.2 mM glucose) with or without insulin (0.1 μ M), using commercial kits at 570 nm. Results were recorded from three independent experiments: *, $P < 0.05$; **, $P < 0.01$; and ***, $P < 0.001$ vs the corresponding control group.

(Figure S1). Compared to vehicle and positive control, **7h** showed significant enhancement on GC/MTT with the effect of insulin, highlighting that **7h** could partly improve insulin sensitivity to further result in marked glucose-lowering effect on insulin-resistant HepG2 cells induced by high glucose culture. Similarly, **7q** exhibited a comparable effect on regulating the glucose consumption to the positive control, and the activity of **7q** was slightly less potent than one of **7h** in vitro.

Inspection of their structural features and activities highlighted that the scaffold of barbituric acid was very profitable for pharmacological activity, and the potencies of thiobarbituric acid derivatives (**8a–g**) were distinctly inferior to those of barbituric acid compounds **7**. The 4-hydroxypiperidine linker of the chemical library of **7** plays critical roles in the activity

compared to the other series of **12**, **14**, and **17**. As for compounds **7a–n**, when the substituted group is a hydrogen atom at the R₁ position, the introduction of different substituted benzamides at the R₂ position improved the glucose-lowering effect compared to pyridine groups. The analysis from the data of **7g–h** indicated that the trifluoromethyl group in the phenyl ring of the R₂ position seemed to be very crucial for the activity.²³ However, the analysis for **7o–z** stated that the cyanopyridine group contributed to the glucose-lowering activity when the fluorine atom was introduced into the R₂ site.

The functions of adipocytes and adipokines, as potential therapeutic targets, play pivotal roles in obese and obesity-related NAFLD. In the study, the mature 3T3-L1 adipocytes

were first obtained by the induction and differentiation of preadipocytes evidenced by H&E staining during 8–12 days. After being cocultured with selected novel barbituric acid derivatives at 10 μM for 24 h, the expression of adiponectin and leptin in 3T3-L1 adipocytes was measured by commercial ELISA kits (Figure 3). Consistent with the glucose-lowering

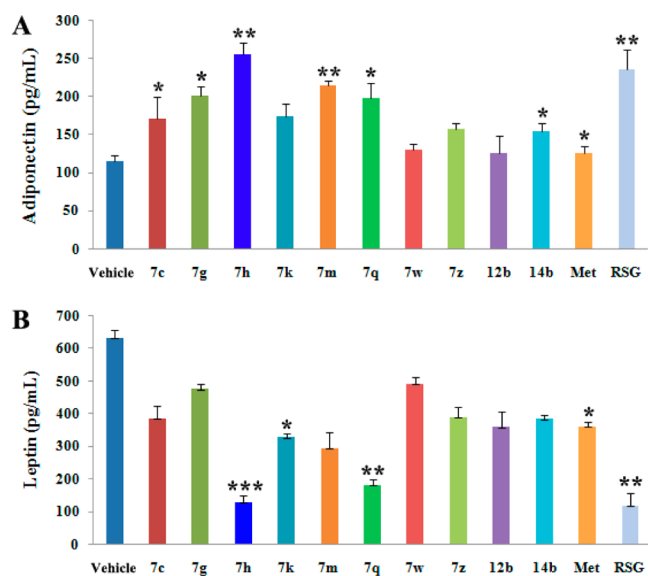


Figure 3. Determination of adiponectin and leptin in 3T3-L1 adipocytes. Rosiglitazone (RSG) and selected compounds at 10 μM and 1.0 mM metformin (Met) were tested in 3T3-L1 adipocytes, using commercial kits (BOSTER, Wuhan, China). Results were recorded from three independent experiments: *, $P < 0.05$; **, $P < 0.01$; and ***, $P < 0.001$ vs vehicle.

effects on insulin resistant HepG2 cells, we found that 7h also possessed excellent potency of up-regulating the expression of adiponectin (122.9% increase from 115.0 pg/mL for vehicle to 256.3 pg/mL for 7h) and down-regulating the secretion of leptin (386.9% decrease from 632.0 pg/mL for vehicle to 129.8 pg/mL for 7h) in 3T3-L1 adipocytes, which were comparable or superior to two standard drugs rosiglitazone (236.0 and 118.8 pg/mL for adiponectin and leptin, respectively) and metformin (125.8 and 360.8 pg/mL). Although 7q exhibited lower potency of regulating the adiponectin expression than 7h and rosiglitazone, 7q effectively down-regulated the leptin level in 3T3-L1 adipocyte with a significant statistic difference. However, 7c, 7g, and 7m could promote the secretion of adiponectin and failed to lower the level of adipocyte-secreted leptin. In contrast, 7h and 7q exhibited more potent activities to modulate the expression of adipokines (adiponectin and leptin) in adipocytes than the other derivatives, with 7h being the most efficacious.

Effects of 7h and 7q on HFD-Induced NAFLD. On the basis of their excellent in vitro potency of regulating GC and the expression of adipokines, 7h and 7q were selected for further in vivo pharmacological evaluation. The two compounds were assessed for their abilities to improve the progression of high fat diet (HFD, 50.55% of calories derived from fat) induced NAFLD in male Wistar rats, a chronic liver disease model that developed obese and obesity-related metabolic features. As for vehicle rats, the mean body weight gain by the reduction for 4 weeks was increased with a statistical difference in contrast to that of normal rats ($P < 0.01$), indicating that the animal NAFLD model was successfully established (Figure 4A). In the acute toxicity test, the male Wistar rats were safe when they were orally administrated to 7h and 7q at a high dosage of 5 g/kg (not

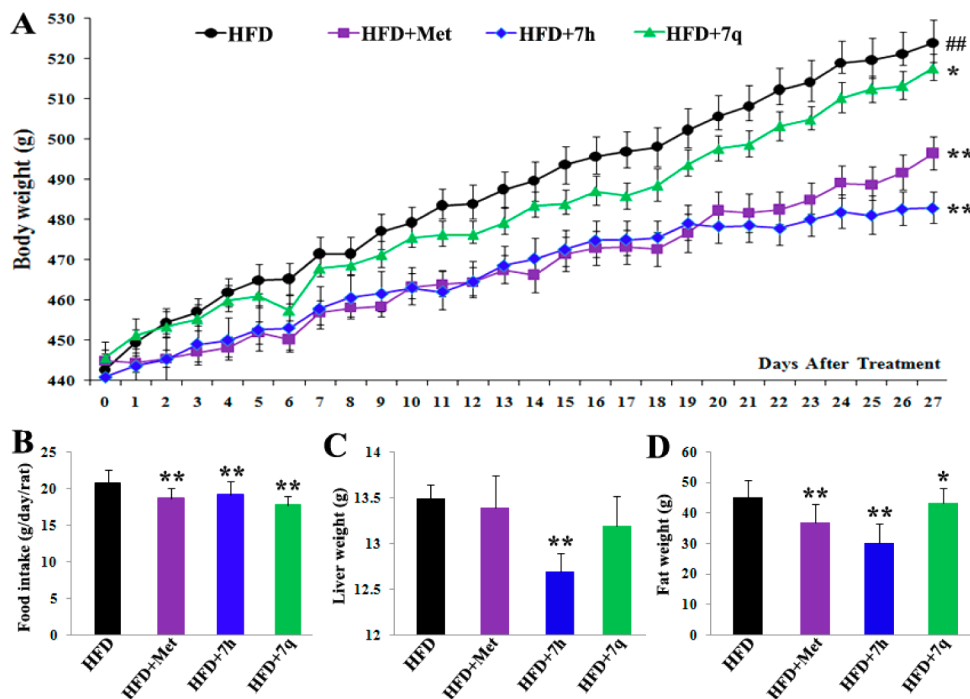


Figure 4. 7h and 7q ameliorate metabolic symptoms in HFD-induced NAFLD model. (A) Body weights of NAFLD rats, either HFD-fed or treated groups ($n = 10$), were monitored during the oral administration of metformin (Met, 150 mg $\text{kg}^{-1} \text{ day}^{-1}$), 7h (25 mg $\text{kg}^{-1} \text{ day}^{-1}$), and 7q (25 mg $\text{kg}^{-1} \text{ day}^{-1}$) for 4 weeks. (B) Food intake, (C) liver weight, and (D) fat weight (epididymal and abdominal fat mass): ##, $P < 0.01$ vs normal group; *, $P < 0.05$; **, $P < 0.01$ vs the corresponding model group.

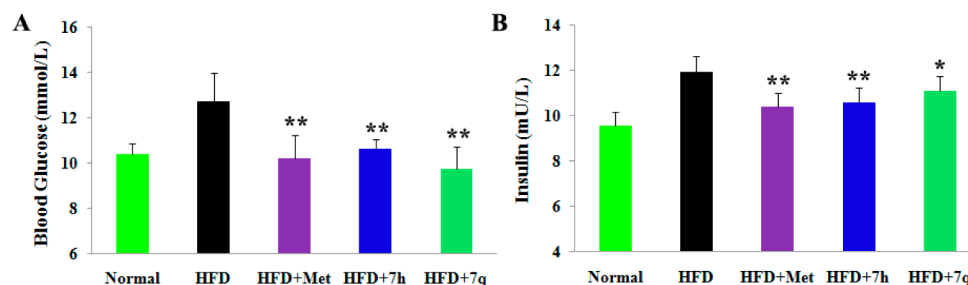


Figure 5. 7h and 7q improve fasting blood glucose and insulin levels in NAFLD. The HFD-fed and treated groups ($n = 10$) were monitored during the oral administration of Met ($150 \text{ mg kg}^{-1} \text{ day}^{-1}$), 7h ($25 \text{ mg kg}^{-1} \text{ day}^{-1}$), and 7q ($25 \text{ mg kg}^{-1} \text{ day}^{-1}$) for 4 weeks. (A) Serum levels of glucose and (B) insulin were determined using insulin kits and a glucometer (Accu Check, Roche), respectively. The results were expressed as the mean \pm SD: *, $P < 0.05$; **, $P < 0.01$ vs HFD group.

Table 3. Parameters of Serum Biochemical Markers from NAFLD Rats^a

parameter	HFD	HFD + Met	HFD + 7h	HFD + 7q
triglycerides (mmol/L)	1.85 \pm 0.14	1.60 \pm 0.15*	1.25 \pm 0.05**	1.70 \pm 0.14*
ALT (U/L)	47.0 \pm 1.5	39.0 \pm 1.9*	33.0 \pm 0.8**	41.0 \pm 3.3*
AST (U/L)	130.0 \pm 5.4	89.0 \pm 3.5*	105.0 \pm 4.8*	140.0 \pm 18.1
total cholesterol (mmol/L)	2.37 \pm 0.03	1.99 \pm 0.03**	1.98 \pm 0.07*	2.02 \pm 0.08*
LDL-c (mmol/L)	0.19 \pm 0.01	0.15*	0.12 \pm 0.01**	0.16 \pm 0.02*
HDL-c (mmol/L)	0.33 \pm 0.01	0.28 \pm 0.01*	0.22 \pm 0.01*	0.25 \pm 0.01**
adiponectin ($\mu\text{g/mL}$)	110.5 \pm 21.3	198.3 \pm 10.2**	213.9 \pm 18.4*	163.3 \pm 21.9
leptin (ng/mL)	20.2 \pm 1.4	13.6 \pm 0.9*	14.1 \pm 1.0*	17.1 \pm 1.6

^aThe HFD-fed ($n = 10$) or treated groups ($n = 10$) were respectively monitored during the oral administration of Met ($150 \text{ mg kg}^{-1} \text{ day}^{-1}$), 7h ($25 \text{ mg kg}^{-1} \text{ day}^{-1}$), and 7q ($25 \text{ mg kg}^{-1} \text{ day}^{-1}$) for 4 weeks. The results were expressed as the mean \pm SD. * $P < 0.05$ vs HFD group. ** $P < 0.01$ vs HFD group.

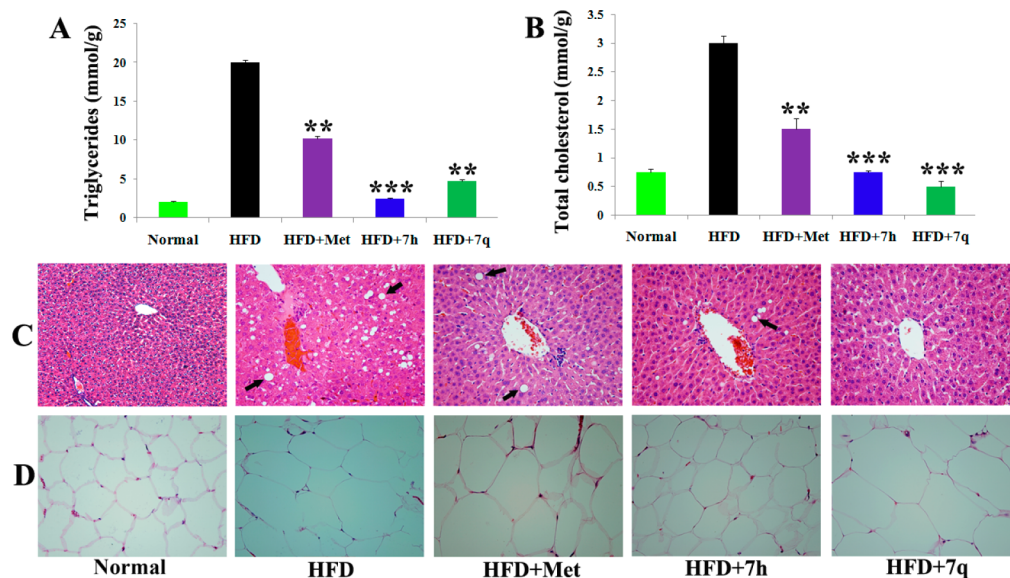


Figure 6. Effects of 7h and 7q on hepatic biochemical markers and H&E staining of liver and adipose tissue from NAFLD rats: (A) content of triglycerides; (B) total cholesterol in liver. The results were expressed as the mean \pm SD ($n = 10$): *, $P < 0.05$; **, $P < 0.01$; and ***, $P < 0.001$ vs HFD group. (C, D) H&E stainings of liver and fat tissue from NAFLD rats (scale, 200 \times). Lipid droplets were marked using the black arrowheads.

shown). By the combination of the results of in vitro assay and previous experimental dosage,¹⁷ we accepted a dose of $25 \text{ mg kg}^{-1} \text{ day}^{-1}$ as a therapeutic strategy. After oral administration of HFD + 7h ($25 \text{ mg kg}^{-1} \text{ day}^{-1}$), HFD + 7q ($25 \text{ mg kg}^{-1} \text{ day}^{-1}$), and HFD + Met ($150 \text{ mg kg}^{-1} \text{ day}^{-1}$) for another 4 weeks, the mean body weight was reduced by the loss values of 7.8%, 1.2%, and 5.2%, respectively, and the cumulative food intakes of treated groups were not affected (Figure 4A,B). Importantly, the mean loss of liver weight by the treatment of 7h, 7q, and

metformin was 5.9%, 0.7%, and 2.2%, respectively, and the mean fat mass loss (abdominal and epididymal) was 30.9%, 4.0%, and 18.1%, respectively (Figure 4C,D), which indicated the reduction of fat deposition in liver and the degradation in adipose tissue. From these data, we summarized that 7q exhibited lower potency of controlling the weight of body, liver, and fat than 7h and metformin at the different dosage, with 7h being the most efficacious at the end of treatment.

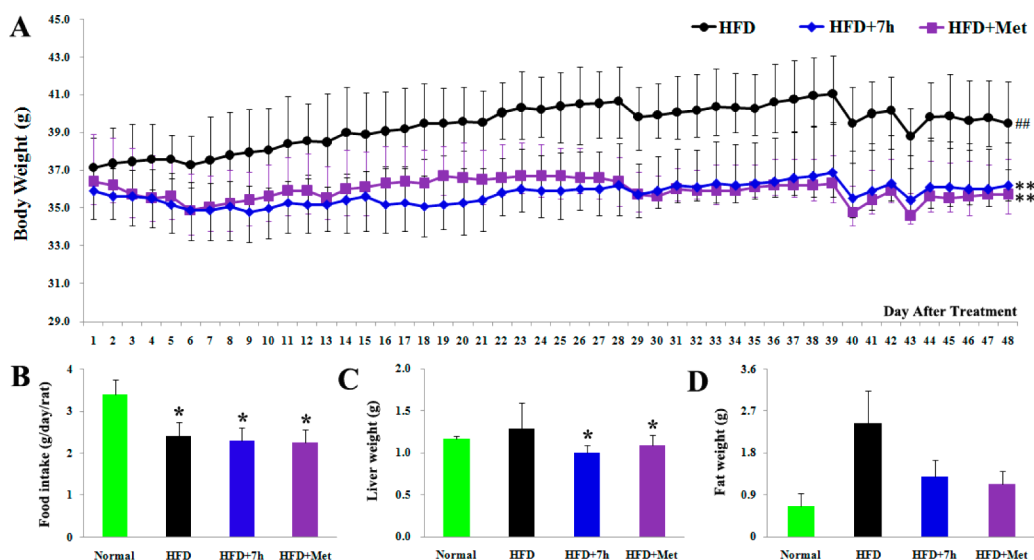


Figure 7. 7h improved the metabolic symptoms in DIO mice. (A) Body weights of DIO mice, either HFD group ($n = 10$) or treated groups ($n = 10$), were monitored during the oral administration of metformin ($150 \text{ mg kg}^{-1} \text{ day}^{-1}$) and 7h ($25 \text{ mg kg}^{-1} \text{ day}^{-1}$) for 7 weeks. (B) Food intake, (C) liver weight, and (D) fat weight (epididymal and abdominal fat mass) were analyzed: ##, $P < 0.01$ vs normal group; *, $P < 0.05$; **, $P < 0.01$ vs the corresponding HFD group.

Because of the fact that blood glucose and insulin played a key role in glucose homeostasis and fat metabolism, we further evaluated serum levels of the two parameters in an HFD-induced NAFLD animal model. As shown in Figure 5, the levels of glucose and insulin were induced to increase during the high fat diet which was orally administrated to the rats for 4 weeks. After the treatment of metformin, 7h, and 7q, the concentration of fasting blood glucose was reduced by 19.7%, 16.3%, and 23.4%, and the serum levels of insulin were decreased by 12.8%, 16.7%, and 6.8%, respectively.

Concurrently, we also measured another six serum levels of triglycerides, AST, ALT, total cholesterol, LDL-c, and HDL-c, which are closely related to fat liver and cardiovascular disease. As exhibited in Table 3, compared to the data of HFD groups, 7h could significantly improve the serum concentrations of triglycerides, ALT, AST, total cholesterol, LDL-c, and HDL-c by 32.4%, 29.8%, 19.2%, 16.5%, 36.8%, and 33.3%, respectively. Similar to the *in vitro* results, 7h also regulated the serum levels of adiponectin and leptin. In contrast, 7h showed more potent ability of regulating HFD-induced abnormal serum biomarkers (triglycerides, AST, ALT, total cholesterol, LDL-c, HDL-c, adiponectin, and leptin) than metformin and 7q.

We found that the content of triglycerides, total cholesterol, and lipid droplets in the liver tissues was significantly increased after the rats had access to a high fatty diet, suggesting that the diet feeding led to an excessive fat deposition, accumulation, and steatosis in liver (Figure 6). In the treated groups, the reduction of hepatic triglycerides by the administration of metformin, 7h, and 7q was 48.8%, 87.5%, and 76.3%, and the decreased content of total cholesterol was 50.0%, 75.0%, and 83.3%, respectively (Figure 6A,B). Interestingly, 7h exhibited slight potency compared with 7q on the reduction of hepatic triglycerides, and 7q was slightly superior to 7h in the regulation of total cholesterol in liver tissue.

As shown in Figure 6C, there were nearly no obvious histological changes and site of steatosis in normal liver sections. However, numerous lipid droplets in liver tissues from HFD-induced rats severely ruined liver histology presented as ballooning degeneration and further led to the formation of

steatosis. Fortunately, the fat accumulation from liver tissues of treated rats (HFD + Met, HFD + 7h, and HFD + 7q) was distinctly alleviated by H&E stainings, and the remarkable reduction of the number and size of lipid droplets was observed (black arrowheads). This result was accorded with a decline in the content of triglycerides and cholesterol in liver. At the same time, no obvious histological changes and toxicity were detected in H&E stainings of liver from normal Wistar rats, which were orally administrated 7h at $25 \text{ mg kg}^{-1} \text{ day}^{-1}$ for 1 week (not shown).

The adipocytes play a critical role in obese and obesity-related diseases. The size of adipocyte elicited from adipose tissues was also ascertained by H&E staining. It was observed that NAFLD rat had a remarkable augmentation in adipocyte size compared to the normal ones, which were significantly restricted after the treatment with 7h (Figure 6D). However, metformin and 7q did not exhibit potent ability of controlling the size of adipocyte and further affected the regulation of the body weight.

Effects of 7h on Diet-Induced Obesity. With the promising anti-NAFLD activities in hand, antiobesity effect of 7h at a dose of 25 mg/kg was further evaluated in diet-induced obesity (DIO) mice. Oral administration of HFD (60.0% of calories derived from fat) in C57BL/6J mice for 8 weeks induced marked obesity as evidenced by the gain of body weight compared to normal ones (BMI as an evaluated reference, $P < 0.01$). After the treatment with 7h for 7 weeks, the mean body weights of HFD-fed mice were significantly reduced (Figure 7A, the mean weight loss of 8.35% at $25 \text{ mg kg}^{-1} \text{ day}^{-1}$) in contrast to ones of HFD ($P < 0.01$) without affecting dramatic changes in accumulative food intake (Figure 7B) and reached similar levels of the metformin-treated group (the mean weight loss of 9.62% at $150 \text{ mg kg}^{-1} \text{ day}^{-1}$). In addition, the mean mass of liver and fat (epididymal and abdominal) was decreased (Figure 7C,D).

The analysis of serum levels of HFD-administered mice indicated significant increase in selected biochemical makers, and the augmentation of these parameters also aggravated the progression of obesity. Compared to the data from HFD

Table 4. Parameters of Biochemical Markers from DIO Mice^a

parameter	normal	HFD	HFD + 7h	HFD + Met
glucose (mmol/L) ^b	8.96 ± 0.68	8.90 ± 1.15	8.02 ± 0.67**	7.98 ± 0.58**
ALT (U/L)	20.01 ± 4.10	85.80 ± 18.21	30.83 ± 5.60*	29.20 ± 8.60*
triglycerides (mmol/L)	0.75 ± 0.17	1.88 ± 0.23	1.04 ± 0.20*	1.33 ± 0.44*
LDL-c (mmol/L)	0.18 ± 0.05	0.36 ± 0.10	0.27 ± 0.09*	0.20*
HDL-c (mmol/L)	0.04 ± 0.01	0.15 ± 0.05	0.09 ± 0.03*	0.08 ± 0.04
FFA (μmol/L)	23.54 ± 0.77	28.38 ± 1.71	25.16 ± 0.87*	27.33 ± 1.08

^aThe HFD-fed group ($n = 10$) or treated groups ($n = 10$) were monitored during the oral administration of metformin ($150 \text{ mg kg}^{-1} \text{ day}^{-1}$), and 7h ($25 \text{ mg kg}^{-1} \text{ day}^{-1}$) for 7 weeks. The results were expressed as the mean ± S.D. ^bFasting blood glucose. *, $P < 0.05$; **, $P < 0.01$ vs HFD group.

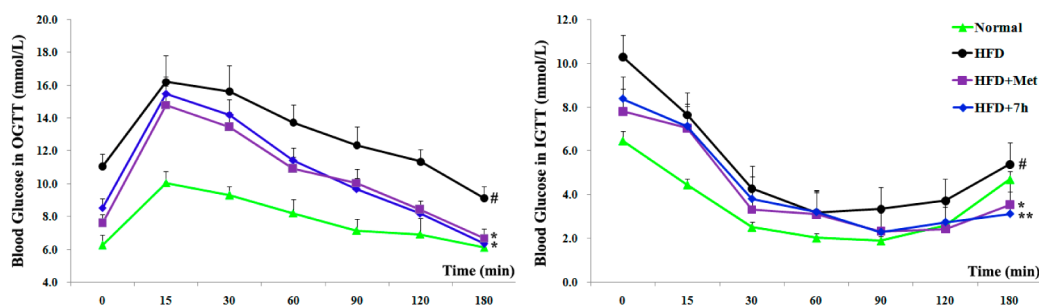


Figure 8. Effects of 7h on postprandial glucose levels in OGTT and IGTT. The two tests were performed using 7h-treated DIO mice ($n = 5$) for 6 weeks after 1 night of fasting. Blood was sampled from the tail vein of mice at 0, 15, 30, 60, 90, 120, and 180 min after an oral glucose load of 3.0 g/kg or intravenous glucose load of 0.5 g/kg of body weight. (A) Blood glucose level in OGTT and (B) blood glucose level in IGTT: #, $P < 0.05$ vs normal group; *, $P < 0.05$; **, $P < 0.01$ vs HFD group.

groups, treatment of 7h and metformin effectively suppressed the serum levels of glucose (9.9%, and 10.3%, respectively), ALT (64.1%, and 66.0%), triglycerides (44.7%, and 29.3%), LDL-c (25.0%, and 44.4%), HDL-c (40.0%, and 46.7%), and free fatty acids (FFA, 11.3%, and 3.7%), with 7h being comparable to metformin at the respective dose (Table 4 and Table S2). In summary, 7h possessed the potential for weight-lowering effect on obese symptoms and improved the obesity-related metabolic features.

On the basis that 7h effectively regulated the levels of blood glucose in NAFLD and DIO animal model, we next investigated the effects of 7h on oral glucose tolerance test (OGTT) and intravenous glucose tolerance test (IGTT). Treatment with 7h at $25 \text{ mg kg}^{-1} \text{ day}^{-1}$ for 6 weeks could inhibit the increase in postprandial glucose level after glucose load intake and improve glucose tolerance in OGTT and IGTT, comparable to that of the standard drug metformin (Figure 8). Because of similar effects on regulating the levels of postprandial glucose, we will further evaluate the potential potency against obesity-related NAFLD by combination therapy of 7h with metformin in the future.

Further, we also investigated the pharmacokinetics of 7h in Sprague–Dawley rats. After oral administration of 7h at a dose of 50 mg/kg , $t_{1/2}$, C_{max} , and T_{max} were 5.3 h, 31.3 μg/L , and 8.0 h, respectively, with the oral bioavailability being 13.9% (Table S3 in Supporting Information). However, the low oral bioavailability may lead to a relative high oral drug dosage in the animal model of obesity-related NAFLD (25 mg/kg), and further structural modification of 7h is in progress.

CONCLUSION

In this study, 54 novel small-molecule (thio)barbituric acid compounds have been designed, synthesized, and evaluated for pharmacological activity. At 10 μM , 7h was found to possess potent glucose-lowering effect on insulin-resistant HepG2 cells

in the presence of insulin (0.1 μM) and regulated the expression of adiponectin and leptin in 3T3-L1 adipocytes. Importantly, oral administration of 7h, at a dose of $25 \text{ mg kg}^{-1} \text{ day}^{-1}$ for 4 weeks, improved effectively the progression of NAFLD by reducing the weight of body, liver, and fat, as well as modulating serum parameters of fasting glucose, insulin, triglycerides, LDL-c, HDL-c, ALT, AST, and hepatic contents of triglycerides, total cholesterol. The results of H&E stainings also revealed that 7h reduced fat deposition in liver tissues and suppressed the increase of adipocyte size in adipose tissues from NAFLD rats. 7h at a single dose of $25 \text{ mg kg}^{-1} \text{ day}^{-1}$ alleviated the clinical symptoms of obesity and regulated serum biomarkers to appropriate ranges, and this compound displayed similar effects as metformin related to glucose tolerance by OGTT and IGTT in DIO mice. These compelling pharmacological profiles might help us to demonstrate that 7h as a candidate constitutes an attractive approach to the treatment of obesity-related NAFLD and is valued for further development. In addition, the detailed pharmacological profiles of 7h and the combination therapy of 7h with metformin are in progress.

EXPERIMENTAL SECTION

Chemistry. Chemical reagents of analytical grade were purchased from Chengdu Changzheng Chemical Factory (Sichuan, P. R. China). TLC was performed on 0.20 mm silical gel 60 F₂₅₄ plates (Qingdao Ocean Chemical Factory, Shandong, China). Hydrogen nuclear magnetic resonance spectra (¹H NMR) were recorded at 400 MHz on a Varian spectrometer (Varian, Palo Alto, CA, U.S.) model Gemini 400 and reported in parts per million. Chemical shifts (δ) are quoted in ppm relative to tetramethylsilane (TMS) as an internal standard, where (δ) TMS = 0.00 ppm. The multiplicity of the signal is indicated as s, singlet; brs, broad singlet; d, doublet; t, triplet; q, quartet; m, multiplet, defined as all multiplex signals where overlap or complex coupling of signals makes definitive descriptions of peaks difficult. Mass spectra (MS) were measured by Q-TOF Premier mass spectrometer utilizing electrospray ionization (ESI) (Micromass, Manchester, U.K.). Room temperature (rt) is within the range 20–

25 °C. The purity was analyzed by HPLC system (Waters 2695, separations module) with a photodiode array detector (Waters 2996, Milford, MA, U.S.), and the chromatographic column was a reversed phase C18 column (Waters, 150 mm × 4.6 mm, i.d. 5 μm). All compounds were supplied in HPLC degree methanol with 10 μL, which was injected on a partial loop, with isocratic elution with 50% acetonitrile and 50% water (containing 0.1% formic acid) at a flow rate of 1 mL/min. The purity of all tested compounds was ≥95% according to our analytical HPLC method.

tert-Butyl 4-(Tosyloxy)piperidine-1-carboxylate (2). A solution of *tert*-butyl 4-hydroxypiperidine-1-carboxylate **1** (1.0 g, 5.0 mmol) in 15 mL of dry pyridine was stirred at 0 °C for 10 min, and a solution of TsCl (1.4 g, 7.5 mmol) in 20 mL of dry pyridine was added slowly. The mixture was stirred at room temperature for 6 h and poured into ice–water. And then the precipitate was collected by filtration, washed with water, and dried in vacuo to afford 80.7% of compound **2**. White solid. ¹H NMR (400 MHz, CDCl₃): δ 7.83 (d, 2H, *J* = 8.4 Hz), 7.38 (d, 2H, *J* = 8.0 Hz), 4.72–4.67 (m, 1H), 3.64–3.58 (m, 2H), 3.30–3.24 (m, 2H), 2.47 (s, 3H), 1.82–1.76 (m, 2H), 1.74–1.66 (m, 2H), 1.45 (s, 9H). MS (ESI), *m/z*: 378.20 [M + Na]⁺.

General Procedure for the Synthesis of 5. A mixture of **2** (1.78 g, 5.0 mmol), appropriate 4-hydroxybenzaldehydes **3** (5.5 mmol), and K₂CO₃ (1.38 g, 10.0 mmol) in 15 mL of DMF was heated to 100 °C for 10 h. And then the K₂CO₃ was removed by filtration. The filtrate was poured into ice–water and extracted with CH₂Cl₂, saturated NaHCO₃, and brine, and the combined organic layer was dried over MgSO₄. Finally, the solvent was removed under reduced pressure to give the crude products **4**. A solution of **4** (1.0 mmol) in 1 mL of TFA/CH₂Cl₂ (*v/v* = 1/1) at 0 °C was stirred for 3 h and allowed to warm to room temperature. After the reaction was completed, the solvent was removed under reduced pressure. The residue was slowly basified with 2 N NaOH, and the solid was formed. The precipitate was collected by filtration and washed with water to afford the crude products **5** without further purification.

General Procedure A for the Synthesis of Amides 6, 9, 13, and 16. Compounds **5** (1.0 mmol), appropriate benzoic acid (1.2 mmol), EDCI (219.2 mg, 1.22 mmol), and DMAP (13.5 mg, 0.11 mmol) were dissolved in 5 mL of CH₂Cl₂. The mixture was stirred at room temperature overnight. After the reaction was completed, water was added into the solution. The solution was extracted with CH₂Cl₂, washed with water and brine, and dried with anhydrous Na₂SO₄. Then the solvent was removed under reduced pressure. The residue was purified by column chromatography on silica gel to afford the target compounds **6**.

General Procedure B for the Synthesis of N-Substituted 6, 9, and 15. To a solution of *tert*-butyl piperidin-4-ylcarbamate (5.0 mmol) and R₁Cl (5.0 mmol) in DMF (15 mL) was added K₂CO₃ (2.07 g, 15.0 mmol). The mixture was heated to 100 °C for 5–18 h. After the mixture was cooled to room temperature, the K₂CO₃ was removed by filtration. The filtrate was poured into water, extracted with EtOAc, washed with water and brine, and dried over MgSO₄. Then the solvent was removed under reduced pressure. The residue was purified by column chromatography on silica gel to afford the target compounds **9**.

General Procedure for the Synthesis of 10. To a solution of **9** (1.0 mmol) in CH₂Cl₂ (1 mL) was added TFA (1 mL) at 0 °C. The resulting brownish solution was allowed to warm to room temperature and stirred for 3 h. And then the mixture was concentrated in vacuo to afford a brown oil residue. The residue was treated with diethyl ether (50 mL) to give a white solid which was collected by filtration. A mixture of the trifluoroacetate solid (5.0 mmol), anhydrous K₂CO₃ (1.38 g, 10.0 mmol) in 10 mL of water, and 30 mL of ethanol was stirred at room temperature for 10 min. 4-(Diethoxymethyl)benzaldehyde (1.0 mL, 5.0 mmol) dissolved into 15 mL of ethanol was added dropwise, and then the mixture was heated to 80 °C overnight. The cooled mixture was extracted with CH₂Cl₂ and water. The organic layer was washed with brine and dried over anhydrous Na₂SO₄. Then the solvent was removed under reduced pressure. The crude was treated in 30 mL of absolute methanol at 0 °C with NaBH₄ (378 mg, 10.0 mmol) in small portion. The mixture was refluxed for

0.5 h and cooled in an ice bath. The mixture was quenched by the addition of 1 N HCl and poured into water (50 mL), and the solution was basified to pH 8–9 with aqueous NaOH. Finally, the formed solid was collected by filtration without further purification.

General Procedure C for the Synthesis of 11a–k and 11n–p. R₂COCl or R₂SO₂Cl (2.0 mmol) was added to a solution of **10** (2.0 mmol) and Et₃N (834 μL, 6.0 mmol) in CH₂Cl₂ (10 mL), and the mixture was stirred at room temperature overnight. Then the solvent was removed under reduced pressure and the residue was purified by column chromatography on silica gel to afford the target compounds.

General Procedure D for the Synthesis of 11l and 11m. Iso(thio)cyanate (2.0 mmol) or (R₂CO)₂O (24 mmol) was added to a solution of **10** (2.0 mmol) in pyridine (10 mL) and stirred at room temperature overnight. Then the solvent was removed under reduced pressure. The residue was purified by column chromatography on silica gel to afford the target compounds.

General Procedure for the Synthesis of 7, 8, 12, 14, and 17. Appropriate aldehydes (0.5 mmol), ethanol (3 mL), distilled water (3 mL), and (thio)barbituric acid (3.0 mmol) were refluxed at 80 °C for 8–24 h. The formed solids were collected by filtration and washed with boiling water (3 × 15 mL), ethanol (3 × 15 mL), and ether (3 × 15 mL). The obtained solids were dried in vacuo for 24 h.

5-(4-(1-Isonicotinoylpiperidin-4-yloxy)benzylidene)pyrimidine-2,4,6(1H,3H,5H)-trione (7a). Yield: 87.9%. HPLC purity: 98.1%. Light yellow solid. ¹H NMR (400 MHz, DMSO-*d*₆): δ 11.31 (s, 1H), 11.18 (s, 1H), 8.68 (d, 2H, *J* = 11.2 Hz), 8.38 (d, 2H, *J* = 8.8 Hz), 8.24 (s, 1H), 7.44 (d, 2H, *J* = 9.6 Hz), 7.13 (d, 2H, *J* = 9.2 Hz), 4.90–4.86 (m, 1H), 4.04–4.01 (m, 1H), 3.48–3.45 (m, 2H), 3.29–3.24 (m, 1H), 2.09–2.07 (m, 1H), 1.97–1.95 (m, 1H), 1.73–1.65 (m, 2H). MS (ESI), *m/z*: 421.11 [M + H]⁺.

5-(4-(1-Nicotinoylpiperidin-4-yloxy)benzylidene)pyrimidine-2,4,6(1H,3H,5H)-trione (7b). Yield: 86.7%. HPLC purity: 99.2%. Light yellow solid. ¹H NMR (400 MHz, DMSO-*d*₆): δ 11.31 (s, 1H), 11.18 (s, 1H), 8.60 (dd, 1H, *J* = 1.2 Hz, *J* = 4.0 Hz), 8.38 (d, 2H, *J* = 9.2 Hz), 8.24 (s, 1H), 7.95 (td, 1H, *J* = 1.6 Hz, *J* = 8.0 Hz), 7.60 (d, 1H, *J* = 7.6 Hz), 7.50 (qd, 1H, *J* = 0.8 Hz, *J* = 4.8 Hz), 7.14 (d, 2H, *J* = 8.8 Hz), 4.91–4.87 (m, 1H), 4.07–4.03 (m, 1H), 3.62–3.59 (m, 1H), 3.52–3.46 (m, 1H), 3.36–3.32 (m, 1H), 2.07–2.02 (m, 1H), 2.00–1.97 (m, 1H), 1.72–1.64 (m, 2H). MS (ESI), *m/z*: 443.14 [M + Na]⁺.

5-(4-(1-Picolinoylpiperidin-4-yloxy)benzylidene)pyrimidine-2,4,6(1H,3H,5H)-trione (7c). Yield: 85.7%. HPLC purity: 97.8%. Light yellow solid. ¹H NMR (400 MHz, DMSO-*d*₆): δ 11.31 (s, 1H), 11.18 (s, 1H), 8.60 (d, 1H, *J* = 4.8 Hz), 8.38 (d, 2H, *J* = 8.8 Hz), 8.24 (s, 1H), 7.95 (t, 1H, *J* = 7.6 Hz), 7.60 (d, 1H, *J* = 7.6 Hz), 7.50 (q, 1H, *J* = 5.2 Hz), 7.14 (d, 2H, *J* = 8.8 Hz), 4.90–4.87 (m, 1H), 4.07–4.03 (m, 1H), 3.62–3.59 (m, 1H), 3.51–3.43 (m, 1H), 3.35–3.33 (m, 1H), 2.10–2.08 (m, 1H), 1.99–1.97 (m, 1H), 1.71–1.64 (m, 2H). MS (ESI), *m/z*: 443.15 [M + Na]⁺.

5-(4-(1-(5-Chloropicolinoyl)piperidine-4-yloxy)benzylidene)pyrimidine-2,4,6(1H,3H,5H)-trione (7d). Yield: 87.7%. HPLC purity: 97.4%. Light yellow solid. ¹H NMR (400 MHz, DMSO-*d*₆): δ 11.31 (s, 1H), 11.18 (s, 1H), 8.58 (d, 1H, *J* = 5.2 Hz), 8.37 (d, 2H, *J* = 8.8 Hz), 8.24 (s, 1H), 7.75 (d, 1H, *J* = 2.0 Hz), 7.65 (dd, 1H, *J* = 2.0 Hz, *J* = 5.2 Hz), 7.13 (d, 2H, *J* = 8.8 Hz), 4.89–4.88 (m, 2H), 4.04–4.01 (m, 1H), 3.59–3.47 (m, 2H), 3.33–3.30 (m, 1H), 2.08–2.06 (m, 1H), 1.99–1.97 (m, 1H), 1.72–1.66 (m, 2H). MS (ESI), *m/z*: 477.15 [M + Na]⁺.

5-(4-(1-(2-Chloroisonicotinoyl)piperidin-4-yloxy)benzylidene)pyrimidine-2,4,6(1H,3H,5H)-trione (7e). Yield: 87.3%. HPLC purity: 99.5%. Light yellow solid. ¹H NMR (400 MHz, DMSO-*d*₆): δ 17.27 (s, 1H), 10.09 (s, 4H), 8.50 (d, 1H, *J* = 5.2 Hz), 7.60 (s, 1H), 7.46 (dd, 1H, *J* = 1.2 Hz, *J* = 5.2 Hz), 6.93 (d, 2H, *J* = 8.0 Hz), 6.79 (d, 2H, *J* = 8.8 Hz), 5.81 (s, 1H), 4.55–4.53 (m, 1H), 3.90–3.88 (m, 1H), 3.51–3.39 (m, 2H), 3.21–3.19 (m, 1H), 2.00–1.97 (m, 1H), 1.88–1.86 (m, 1H), 1.68–1.63 (m, 2H). MS (ESI), *m/z*: 477.14 [M + Na]⁺.

5-(4-(1-(3-(Trifluoromethyl)benzoyl)piperidin-4-yloxy)benzylidene)pyrimidine-2,4,6(1H,3H,5H)-trione (7f). Yield: 84.3%. HPLC purity: 99.0%. Light yellow solid. ¹H NMR (400

MHz, DMSO- d_6): δ 11.31 (s, 1H), 11.19 (s, 1H), 8.38 (d, 2H, $J = 9.2$ Hz), 8.25 (s, 1H), 7.84 (d, 1H, $J = 7.6$ Hz), 7.80 (s, 1H), 7.77 (d, 1H, $J = 7.6$ Hz), 7.71 (d, 1H, $J = 8.0$ Hz), 7.14 (d, 2H, $J = 8.8$ Hz), 4.89–4.87 (m, 1H), 4.04–4.00 (m, 1H), 3.47–3.41 (m, 3H), 2.09–1.97 (m, 2H), 1.74–1.68 (m, 2H). MS (ESI), m/z : 510.09 [M + Na] $^+$.

5-(4-(1-(3-Fluoro-4-(trifluoromethyl)benzoyl)piperidin-4-yloxy)benzylidene)pyrimidine-2,4,6(1H,3H,5H)-trione (7g). Yield: 89.5%. HPLC purity: 97.6%. Light yellow solid. ^1H NMR (400 MHz, DMSO- d_6): δ 11.32 (s, 1H), 11.19 (s, 1H), 8.38 (d, 2H, $J = 8.8$ Hz), 8.25 (s, 1H), 7.90 (t, 1H, $J = 7.6$ Hz), 7.67 (d, 1H, $J = 10.8$ Hz), 7.49 (d, 1H, $J = 8.0$ Hz), 7.14 (d, 2H, $J = 8.8$ Hz), 4.90–4.86 (m, 1H), 4.03–4.01 (m, 1H), 3.49–3.47 (m, 2H), 3.30–3.28 (m, 1H), 2.09–2.07 (m, 1H), 1.98–1.96 (m, 1H), 1.73–1.71 (m, 2H). MS (ESI), m/z : 506.07 [M + H] $^+$.

5-(4-(1-(4-(Difluoromethoxy)benzoyl)piperidin-4-yloxy)benzylidene)pyrimidine-2,4,6(1H,3H,5H)-trione (7h). Yield: 83.4%. HPLC purity: 99.91% (Supporting Information). Light yellow solid. ^1H NMR (400 MHz, DMSO- d_6): δ 11.32 (s, 1H), 11.19 (s, 1H), 8.38 (d, 2H, $J = 8.8$ Hz), 8.25 (s, 1H), 7.52 (d, 2H, $J = 8.4$ Hz), 7.51 (t, 1H, $J = 74.0$ Hz), 7.25 (d, 2H, $J = 8.0$ Hz), 7.14 (d, 2H, $J = 8.8$ Hz), 4.88–4.86 (m, 1H), 4.02–4.00 (m, 1H), 3.56–3.34 (m, 3H), 2.04–2.02 (m, 2H), 1.69–1.67 (m, 2H). ^{13}C NMR (100 MHz, DMSO- d_6): δ 166.1, 163.9, 161.2, 160.0, 157.4, 154.8, 150.2, 143.1, 143.0, 137.5, 127.8, 125.2, 123.2, 123.1, 115.6, 115.5, 115.4, 115.2, 72.1, 44.0, 38.6, 30.5, 29.8. MS (ESI), m/z : 508.22 [M + Na] $^+$.

5-(4-(1-(2-Chloronicotinoyl)piperidin-4-yloxy)benzylidene)pyrimidine-2,4,6(1H,3H,5H)-trione (7i). Yield: 86.2%. HPLC purity: 98.6%. Light yellow solid. ^1H NMR (400 MHz, DMSO- d_6): δ 11.31 (s, 1H), 11.19 (s, 1H), 8.50 (dd, 1H, $J = 1.6$ Hz, $J = 4.8$ Hz), 8.38 (d, 2H, $J = 9.2$ Hz), 8.25 (s, 1H), 7.98 (td, 1H, $J = 1.2$ Hz, $J = 8.0$ Hz), 7.55 (q, 1H, $J = 4.2$ Hz), 7.15 (t, 2H, $J = 8.4$ Hz), 4.90–4.87 (m, 1H), 4.12–4.06 (m, 1H), 3.52–3.48 (m, 1H), 3.34–3.27 (m, 1H), 3.26–3.20 (m, 1H), 2.10–2.08 (m, 1H), 1.98–1.96 (m, 1H), 1.76–1.64 (m, 2H). MS (ESI), m/z : 477.03 [M + Na] $^+$.

5-(4-(1-(4-Nitropyridin-2-yl)piperidin-4-yloxy)benzylidene)pyrimidine-2,4,6(1H,3H,5H)-trione (7j). Yield: 86.2%. HPLC purity: 98.8%. Light yellow solid. ^1H NMR (400 MHz, DMSO- d_6): δ 11.32 (s, 1H), 11.19 (s, 1H), 8.38 (d, 2H, $J = 8.4$ Hz), 8.25 (s, 1H), 7.95 (d, 1H, $J = 5.6$ Hz), 7.14 (d, 2H, $J = 8.8$ Hz), 6.90 (s, 1H), 6.88 (s, 1H), 4.87–4.85 (m, 1H), 3.78–3.74 (m, 2H), 3.31–3.29 (m, 2H), 2.05–2.01 (m, 2H), 1.68–1.65 (m, 2H). MS (ESI), m/z : 438.36 [M + H] $^+$.

5-(4-(1-(5-Nitropyridin-2-yl)piperidin-4-yloxy)benzylidene)pyrimidine-2,4,6(1H,3H,5H)-trione (7k). Yield: 82.1%. HPLC purity: 99.8%. Light yellow solid. ^1H NMR (400 MHz, DMSO- d_6): δ 11.32 (s, 1H), 11.20 (s, 1H), 8.99 (d, 1H, $J = 2.8$ Hz), 8.39 (d, 2H, $J = 8.8$ Hz), 8.25 (s, 1H), 8.24 (dd, 1H, $J = 2.8$ Hz, $J = 9.6$ Hz), 7.16 (d, 2H, $J = 8.8$ Hz), 7.03 (d, 1H, $J = 9.6$ Hz), 4.93–4.92 (m, 1H), 4.17–4.15 (m, 2H), 3.69–4.64 (m, 2H), 2.10–2.08 (m, 2H), 1.72–1.69 (m, 2H). MS (ESI), m/z : 438.24 [M + H] $^+$.

2-(4-(4-(2,4,6-Trioxotetrahydropyrimidin-5(6H)-ylidene)methyl)phenoxy)piperidin-1-yl)nicotinonitrile (7l). Yield: 81.8%. HPLC purity: 99.3%. Light yellow solid. ^1H NMR (400 MHz, DMSO- d_6): δ 11.31 (s, 1H), 11.19 (s, 1H), 8.43 (dd, 1H, $J = 2$ Hz, $J = 4.8$ Hz), 8.39 (d, 2H, $J = 8.8$ Hz), 8.25 (s, 1H), 8.09 (dd, 1H, $J = 1.6$ Hz, $J = 7.6$ Hz), 7.15 (d, 2H, $J = 9.2$ Hz), 6.94 (q, 1H, $J = 7.6$ Hz), 4.90–4.88 (m, 1H), 4.00–3.96 (m, 2H), 3.54–3.49 (m, 2H), 2.12–2.10 (m, 2H), 1.80–1.73 (m, 2H). MS (ESI), m/z : 440.11 [M + Na] $^+$.

5-(4-(1-(3-(Trifluoromethyl)pyridin-2-yl)piperidin-4-yloxy)benzylidene)pyrimidine-2,4,6(1H,3H,5H)-trione (7m). Yield: 86.3%. HPLC purity: 97.9%. Light yellow solid. ^1H NMR (400 MHz, DMSO- d_6): δ 11.31 (s, 1H), 11.18 (s, 1H), 8.54 (d, 1H, $J = 4.4$ Hz), 8.39 (d, 2H, $J = 9.2$ Hz), 8.25 (s, 1H), 8.08 (d, 1H, $J = 8.0$ Hz), 7.21 (q, 1H, $J = 1.2$ Hz), 7.15 (d, 2H, $J = 8.8$ Hz), 4.84–4.82 (m, 1H), 3.48–3.44 (m, 2H), 3.19 (t, 2H, $J = 9.6$ Hz), 2.10–2.09 (m, 2H), 1.80–1.78 (m, 2H). MS (ESI), m/z : 461.15 [M + H] $^+$.

5-(4-(1-(5-(Trifluoromethyl)pyridin-2-yl)piperidin-4-yloxy)benzylidene)pyrimidine-2,4,6(1H,3H,5H)-trione (7n). Yield: 85.1%. HPLC purity: 98.7%. Light yellow solid. ^1H NMR (400 MHz, DMSO- d_6): δ 11.31 (s, 1H), 11.19 (s, 1H), 8.42 (s, 1H), 8.39 (d, 2H, $J = 9.2$ Hz), 8.25 (s, 1H), 7.81 (dd, 1H, $J = 2.4$ Hz, $J = 9.2$ Hz),

7.15 (d, 2H, $J = 8.8$ Hz), 7.04 (d, 1H, $J = 9.2$ Hz), 4.92–4.88 (m, 1H), 4.11–4.06 (m, 2H), 3.53–3.48 (m, 2H), 2.09–2.05 (m, 2H), 1.69–1.62 (m, 2H). MS (ESI), m/z : 461.14 [M + H] $^+$.

5-(3-Fluoro-4-(1-(nicotinoyl)piperidin-4-yloxy)benzylidene)pyrimidine-2,4,6(1H,3H,5H)-trione (7o). Yield: 83.4%. HPLC purity: 97.9%. Light yellow solid. ^1H NMR (400 MHz, DMSO- d_6): δ 17.25 (s, 1H), 10.10 (s, 4H), 8.59 (d, 1H, $J = 4.8$ Hz), 7.93 (td, 1H, $J = 7.6$ Hz, $J = 0.8$ Hz), 7.58 (d, 1H, $J = 7.6$ Hz), 7.48 (q, 1H, $J = 4.2$ Hz), 7.05 (t, 1H, $J = 8.8$ Hz), 6.76 (d, 2H, $J = 10.4$ Hz), 5.86 (s, 1H), 4.53–4.51 (m, 1H), 3.98–3.94 (m, 1H), 3.57–3.44 (m, 2H), 3.29–3.25 (m, 1H), 2.00–1.98 (m, 1H), 1.89–1.87 (m, 1H), 1.67–1.60 (m, 2H). MS (ESI), m/z : 439.25 [M + H] $^+$.

5-(3-Fluoro-4-(1-isonicotinoyl)piperidin-4-yloxy)benzylidene)pyrimidine-2,4,6(1H,3H,5H)-trione (7p). Yield: 86.2%. HPLC purity: 98.6%. Light yellow solid. ^1H NMR (400 MHz, DMSO- d_6): δ 11.37 (s, 1H), 11.26 (s, 1H), 8.68 (d, 2H, $J = 6.0$ Hz), 8.55 (dd, 1H, $J = 1.6$ Hz, $J = 13.2$ Hz), 8.22 (s, 1H), 8.02 (d, 1H, $J = 8.8$ Hz), 7.45 (d, 3H, $J = 6.0$ Hz), 4.94–4.93 (m, 1H), 4.03–3.99 (m, 1H), 3.51–3.46 (m, 2H), 3.29–3.26 (m, 1H), 2.09–2.07 (m, 1H), 1.99–1.97 (m, 1H), 1.77–1.72 (m, 2H). MS (ESI), m/z : 439.31 [M + H] $^+$.

5-(4-(1-(2-Chloronicotinoyl)piperidin-4-yloxy)-3-fluorobenzylidene)pyrimidine-2,4,6(1H,3H,5H)-trione (7q). Yield: 82.1%. HPLC purity: 100% (Supporting Information). Light yellow solid. ^1H NMR (400 MHz, DMSO- d_6): δ 11.38 (s, 1H), 11.26 (s, 1H), 8.55 (d, 1H, $J = 14.0$ Hz), 8.49 (d, 1H, $J = 4.0$ Hz), 8.22 (s, 1H), 8.02 (d, 1H, $J = 8.4$ Hz), 7.99 (t, 1H, $J = 7.2$ Hz), 7.55 (t, 1H, $J = 5.6$ Hz), 7.45 (q, 1H, $J = 8.4$ Hz), 4.95–4.93 (m, 1H), 4.08–4.05 (m, 1H), 3.56–3.47 (m, 1H), 3.35–3.33 (m, 1H), 3.27–3.22 (m, 1H), 2.12–2.10 (m, 1H), 2.00–1.98 (m, 1H), 1.79–1.71 (m, 2H). ^{13}C NMR (100 MHz, DMSO- d_6): δ 163.6, 162.1, 160.2, 153.5, 152.0, 150.1, 149.2, 149.1, 144.3, 133.8, 125.5, 125.4, 121.1, 120.9, 117.9, 116.9, 115.2, 114.6, 94.4, 73.6, 45.1, 30.1. MS (ESI), m/z : 473.53 [M + H] $^+$.

5-(3-Fluoro-4-(1-(3-(trifluoromethyl)benzoyl)piperidin-4-yloxy)benzylidene)pyrimidine-2,4,6(1H,3H,5H)-trione (7r). Yield: 83.7%. HPLC purity: 98.9%. Light yellow solid. ^1H NMR (400 MHz, DMSO- d_6): δ 11.37 (s, 1H), 11.26 (s, 1H), 8.56 (dd, 1H, $J = 1.6$ Hz, $J = 10.0$ Hz), 8.22 (s, 1H), 8.02 (d, 1H, $J = 8.4$ Hz), 7.84 (d, 2H, $J = 10.8$ Hz), 7.78 (d, 1H, $J = 8.0$ Hz), 7.71 (t, 1H, $J = 7.6$ Hz), 7.45 (t, 1H, $J = 8.8$ Hz), 4.94–4.92 (m, 1H), 4.02–4.00 (m, 1H), 3.50–3.48 (m, 2H), 3.35–3.33 (m, 1H), 2.09–1.99 (m, 2H), 1.78–1.74 (m, 2H). MS (ESI), m/z : 506.11 [M + H] $^+$.

5-(3-Fluoro-4-(1-(3-fluoro-4-(trifluoromethyl)benzoyl)piperidin-4-yloxy)benzylidene)pyrimidine-2,4,6(1H,3H,5H)-trione (7s). Yield: 85.7%. HPLC purity: 98.8%. Light yellow solid. ^1H NMR (400 MHz, DMSO- d_6): δ 11.37 (s, 1H), 11.26 (s, 1H), 8.55 (d, 1H, $J = 13.6$ Hz), 8.22 (s, 1H), 8.02 (d, 1H, $J = 8.4$ Hz), 7.89 (t, 1H, $J = 7.6$ Hz), 7.68 (d, 1H, $J = 10.8$ Hz), 7.50 (d, 1H, $J = 8.4$ Hz), 7.45 (t, 1H, $J = 8.8$ Hz), 4.95–4.93 (m, 1H), 3.41–3.98 (m, 1H), 3.47–3.41 (m, 2H), 3.34–3.28 (m, 1H), 2.10–2.07 (m, 1H), 1.99–1.97 (m, 1H), 1.76–1.74 (m, 2H). MS (ESI), m/z : 524.25 [M + H] $^+$.

5-(4-(1-(4-(Difluoromethoxy)benzoyl)piperidin-4-yloxy)-3-fluorobenzylidene)pyrimidine-2,4,6(1H,3H,5H)-trione (7t). Yield: 81.9%. HPLC purity: 98.1%. Light yellow solid. ^1H NMR (400 MHz, DMSO- d_6): δ 11.37 (s, 1H), 11.26 (s, 1H), 8.56 (dd, 1H, $J = 2.0$ Hz, $J = 13.2$ Hz), 8.22 (s, 1H), 8.02 (d, 1H, $J = 7.6$ Hz), 7.53 (d, 2H, $J = 8.4$ Hz), 7.48 (t, 1H, $J = 61.6$ Hz), 7.45 (t, 1H, $J = 8.8$ Hz), 7.25 (d, 2H, $J = 8.8$ Hz), 4.94–4.92 (m, 1H), 4.02–3.98 (m, 1H), 3.55–3.40 (m, 3H), 2.09–2.04 (m, 2H), 1.73–1.71 (m, 2H). MS (ESI), m/z : 526.10 [M + Na] $^+$.

5-(3-Fluoro-4-(1-(3-(1,1,2,2-tetrafluoroethoxy)benzoyl)piperidin-4-yloxy)benzylidene)pyrimidine-2,4,6(1H,3H,5H)-trione (7u). Yield: 82.5%. HPLC purity: 98.4%. Light yellow solid. ^1H NMR (400 MHz, DMSO- d_6): δ 11.37 (s, 1H), 11.26 (s, 1H), 8.56 (dd, 1H, $J = 1.6$ Hz, $J = 14.0$ Hz), 8.22 (s, 1H), 8.02 (d, 1H, $J = 8.4$ Hz), 7.59 (t, 1H, $J = 7.6$ Hz), 7.45 (d, 2H, $J = 8.8$ Hz), 7.40 (d, 1H, $J = 5.2$ Hz), 7.37 (t, 1H, $J = 5.2$ Hz), 6.96 (t, 1H, $J = 1.6$ Hz, $J = 51.6$ Hz), 4.94–4.92 (m, 1H), 3.42–3.38 (m, 1H), 3.48–3.56 (m, 3H), 2.09–2.00 (m, 2H), 1.74–1.73 (m, 2H). MS (ESI), m/z : 576.08 [M + Na] $^+$.

5-(4-(1-(2,2-Difluorobenzo[d][1,3]dioxole-4-carbonyl)-piperidin-4-yloxy)-3-fluorobenzylidene)pyrimidine-2,4,6-(1H,3H,5H)-trione (7v). Yield: 86.1%. HPLC purity: 99.3%. Light yellow solid. ¹H NMR (400 MHz, DMSO-*d*₆): δ 11.38 (s, 1H), 11.27 (s, 1H), 8.56 (dd, 1H, *J* = 1.6 Hz, *J* = 14.0 Hz), 8.23 (s, 1H), 8.02 (d, 1H, *J* = 8.4 Hz), 7.53 (q, 1H, *J* = 3.6 Hz), 7.45 (t, 1H, *J* = 8.8 Hz), 7.31 (dd, 2H, *J* = 1.6 Hz, *J* = 5.2 Hz), 4.96–4.93 (m, 1H), 4.04–4.01 (m, 1H), 3.52–3.50 (m, 2H), 3.36–3.34 (m, 1H), 2.11–2.09 (m, 1H), 2.02–2.00 (m, 1H), 1.75–1.68 (m, 2H). MS (ESI), *m/z*: 540.23 [M + Na]⁺.

2-(4-(2-Fluoro-4-((2,4,6-trioxotetrahydropyrimidin-5(6H)-ylidene)methyl)phenoxy)piperidin-1-yl)nicotinonitrile (7w). Yield: 88.4%. HPLC purity: 98.3%. Light yellow solid. ¹H NMR (400 MHz, DMSO-*d*₆): δ 11.38 (s, 1H), 11.27 (s, 1H), 8.57 (dd, 1H, *J* = 2 Hz, *J* = 13.6 Hz), 8.43 (dd, 1H, *J* = 2 Hz, *J* = 4.8 Hz), 8.23 (s, 1H), 8.10 (dd, 1H, *J* = 2 Hz, *J* = 8 Hz), 8.04 (d, 1H, *J* = 8 Hz), 7.47 (t, 1H, *J* = 8.8 Hz), 6.95 (q, 1H, *J* = 7.6 Hz), 4.96 (m, 1H), 4.00–3.95 (m, 2H), 3.54–3.49 (m, 2H), 2.13–2.09 (m, 2H), 1.83–1.76 (m, 2H). MS (ESI), *m/z*: 436.23 [M + H]⁺.

5-(3-Fluoro-4-(1-(3-(trifluoromethyl)pyridin-2-yl)piperidin-4-yloxy)benzylidene)pyrimidine-2,4,6-(1H,3H,5H)-trione (7x). Yield: 83.4%. HPLC purity: 98.7%. Light yellow solid. ¹H NMR (400 MHz, DMSO-*d*₆): δ 11.37 (s, 1H), 11.27 (s, 1H), 8.57 (d, 2H, *J* = 14.0 Hz), 8.23 (s, 1H), 8.09 (d, 1H, *J* = 7.6 Hz), 8.03 (d, 1H, *J* = 8.4 Hz), 7.46 (t, 1H, *J* = 8.8 Hz), 7.22 (q, 1H, *J* = 4.8 Hz), 4.90–4.89 (m, 1H), 3.47–3.44 (m, 2H), 3.19–3.15 (m, 2H), 2.13–2.11 (m, 2H), 1.85–1.79 (m, 2H). MS (ESI), *m/z*: 479.25 [M + H]⁺.

5-(3-Fluoro-4-(1-(5-(trifluoromethyl)pyridin-2-yl)piperidin-4-yloxy)benzylidene)pyrimidine-2,4,6-(1H,3H,5H)-trione (7y). Yield: 83.4%. HPLC purity: 99.8%. Light yellow solid. ¹H NMR (400 MHz, DMSO-*d*₆): δ 11.38 (s, 1H), 11.27 (s, 1H), 8.56 (d, 1H, *J* = 2.0 Hz, *J* = 13.6 Hz), 8.42 (s, 1H), 8.22 (s, 1H), 8.04 (d, 1H, *J* = 8.8 Hz), 7.82 (dd, 1H, *J* = 2.4 Hz, *J* = 8.8 Hz), 7.47 (t, 1H, *J* = 9.2 Hz), 7.04 (d, 1H, *J* = 9.2 Hz), 4.96–4.95 (m, 1H), 4.10–4.07 (m, 2H), 3.54–3.49 (m, 2H), 2.09–2.06 (m, 2H), 1.72–1.65 (m, 2H). MS (ESI), *m/z*: 479.26 [M + H]⁺.

Methyl 4-(4-(2-Fluoro-4-((2,4,6-trioxotetrahydropyrimidin-5(6H)-ylidene)methyl)phenoxy)piperidin-1-ylsulfonyl)thiophene-3-carboxylate (7z). Yield: 85.1%. HPLC purity: 99.4%. Light yellow solid. ¹H NMR (400 MHz, DMSO-*d*₆): δ 11.37 (s, 1H), 11.26 (s, 1H), 8.52 (dd, 1H, *J* = 2 Hz, *J* = 13.6 Hz), 8.21 (s, 1H), 8.03 (d, 1H, *J* = 5.2 Hz), 7.99 (d, 1H, *J* = 8.8 Hz), 7.49 (d, 1H, *J* = 5.2 Hz), 7.39 (t, 1H, *J* = 8.8 Hz), 4.81–4.77 (m, 1H), 3.86 (s, 3H), 3.55–3.51 (m, 2H), 3.81–3.14 (m, 2H), 2.06–2.03 (m, 2H), 1.73–1.68 (m, 2H). MS (ESI), *m/z*: 560.03 [M + Na]⁺.

5-(4-(1-(5-Methylpyrazine-2-carbonyl)piperidin-4-yloxy)-benzylidene)-2-thioxodihydropyrimidine-4,6-(1H,5H)-dione (8a). Yield: 84.6%. HPLC purity: 97.5%. Light yellow solid. ¹H NMR (400 MHz, DMSO-*d*₆): δ 12.41 (s, 1H), 12.31 (s, 1H), 8.74 (d, 1H, *J* = 1.6 Hz), 8.57 (s, 1H), 8.43 (d, 2H, *J* = 9.2 Hz), 8.27 (s, 1H), 7.16 (d, 2H, *J* = 9.2 Hz), 4.94–4.90 (m, 1H), 4.07–4.03 (m, 1H), 3.68–3.65 (m, 1H), 3.53–3.48 (m, 1H), 3.45–3.39 (m, 1H), 2.55 (s, 3H), 2.10–2.08 (m, 1H), 2.02–2.00 (m, 1H), 1.73–1.67 (m, 2H). MS (ESI), *m/z*: 468.32 [M + H]⁺.

5-(4-(1-(4-Chloro-2-methoxybenzoyl)piperidin-4-yloxy)-benzylidene)-2-thioxodihydropyrimidine-4,6-(1H,5H)-dione (8b). Yield: 82.3%. HPLC purity: 98.1%. Light yellow solid. ¹H NMR (400 MHz, DMSO-*d*₆): δ 12.41 (s, 1H), 12.31 (s, 1H), 8.43 (d, 2H, *J* = 9.2 Hz), 8.26 (s, 1H), 7.46 (dd, 1H, *J* = 2.4 Hz, *J* = 8.8 Hz), 7.32 (dd, 1H, *J* = 2.4 Hz, *J* = 9.2 Hz), 7.16–7.11 (m, 3H), 4.88–4.86 (m, 1H), 4.03–3.99 (m, 1H), 3.81 (s, 3H), 3.45–3.32 (m, 2H), 3.18–3.15 (m, 1H), 2.05–1.93 (m, 2H), 1.69–1.58 (m, 2H). MS (ESI), *m/z*: 516.56 [M + H]⁺.

5-(4-(1-(4-Fluorophenylsulfonyl)piperidin-4-yloxy)-benzylidene)-2-thioxodihydropyrimidine-4,6-(1H,5H)-dione (8c). Yield: 85.2%. HPLC purity: 98.9%. Light yellow solid. ¹H NMR (400 MHz, DMSO-*d*₆): δ 12.40 (s, 1H), 12.30 (s, 1H), 8.37 (d, 2H, *J* = 8.8 Hz), 8.23 (s, 1H), 7.88 (q, 2H, *J* = 5.2 Hz), 7.56 (t, 2H, *J* = 9.2 Hz), 7.06 (d, 2H, *J* = 8.8 Hz), 4.66–4.45 (m, 1H), 3.35–3.31 (m, 2H), 2.84–2.80 (m, 2H), 2.06–2.03 (m, 2H), 1.75–1.68 (m, 2H). MS (ESI), *m/z*: 506.14 [M + H]⁺.

2-Thioxo-5-(4-(1-(5-(trifluoromethyl)pyridin-2-yl)piperidin-4-yloxy)benzylidene)dihydropyrimidine-4,6-(1H,5H)-dione (8d). Yield: 82.8%. HPLC purity: 99.2%. Light yellow solid. ¹H NMR (400 MHz, DMSO-*d*₆): δ 12.41 (s, 1H), 12.31 (s, 1H), 8.44–8.42 (m, 3H), 8.27 (s, 1H), 7.81 (dd, 1H, *J* = 2.4 Hz, *J* = 9.2 Hz), 7.17 (d, 2H, *J* = 9.2 Hz), 7.04 (d, 1H, *J* = 9.2 Hz), 4.93–4.91 (m, 1H), 4.11–4.08 (m, 2H), 3.53–3.48 (m, 2H), 2.06–2.04 (m, 2H), 1.69–1.62 (m, 2H). MS (ESI), *m/z*: 493.25 [M + H]⁺.

5-(3-Ethoxy-4-(1-(3-fluoro-4-(trifluoromethyl)benzoyl)-piperidin-4-yloxy)benzylidene)-2-thioxodihydropyrimidine-4,6-(1H,5H)-dione (8e). Yield: 81.6%. HPLC purity: 99.5%. Light yellow solid. ¹H NMR (400 MHz, DMSO-*d*₆): δ 12.42 (s, 1H), 12.30 (s, 1H), 8.45 (d, 1H, *J* = 1.6 Hz), 8.26 (s, 1H), 7.92 (q, 2H, *J* = 7.6 Hz), 7.69 (d, 1H, *J* = 10.8 Hz), 7.50 (d, 1H, *J* = 8.0 Hz), 7.27 (d, 1H, *J* = 8.8 Hz), 4.89–4.87 (m, 1H), 4.12 (q, 2H, *J* = 7.2 Hz), 4.02–3.99 (m, 1H), 3.49–3.47 (m, 2H), 3.29–3.24 (m, 1H), 2.10–2.08 (m, 1H), 1.99–1.95 (m, 1H), 1.74–1.72 (m, 2H), 1.39 (t, 3H, *J* = 7.2 Hz). MS (ESI), *m/z*: 582.32 [M + H]⁺.

2-(4-(4-((4,6-Dioxo-2-thioxotetrahydropyrimidin-5(6H)-ylidene)methyl)-2-ethoxyphenoxy)piperidin-1-yl)nicotinonitrile (8f). Yield: 82.4%. HPLC purity: 99.8%. Light yellow solid. ¹H NMR (400 MHz, DMSO-*d*₆): δ 12.42 (s, 1H), 12.31 (s, 1H), 8.46 (s, 1H), 8.43 (dd, 1H, *J* = 1.6 Hz, *J* = 4.8 Hz), 8.27 (s, 1H), 8.10 (d, 1H, *J* = 8.0 Hz), 7.94 (d, 1H, *J* = 8.8 Hz), 7.29 (d, 1H, *J* = 8.8 Hz), 6.94 (q, 1H, *J* = 4.8 Hz), 4.91–4.89 (m, 1H), 4.12 (q, 2H, *J* = 7.2 Hz), 3.99–3.95 (m, 2H), 3.54–3.50 (m, 2H), 2.10–2.08 (m, 2H), 1.81–1.77 (m, 2H), 1.38 (t, 3H, *J* = 6.8 Hz). MS (ESI), *m/z*: 494.16 [M + H]⁺.

2-(4-(4-((4,6-Dioxo-2-thioxotetrahydropyrimidin-5(6H)-ylidene)methyl)-2,6-dimethoxyphenoxy)piperidin-1-yl)nicotinonitrile (8g). Yield: 83.7%. HPLC purity: 98.4%. Light yellow solid. ¹H NMR (400 MHz, DMSO-*d*₆): δ 12.47 (s, 1H), 12.37 (s, 1H), 8.42 (dd, 1H, *J* = 1.6 Hz, *J* = 4.8 Hz), 8.30 (s, 1H), 8.08 (dd, 1H, *J* = 2.0 Hz, *J* = 7.6 Hz), 7.94 (s, 2H), 6.92 (q, 1H, *J* = 4.8 Hz), 4.57–4.55 (m, 1H), 3.94–3.90 (m, 2H), 3.84 (s, 6H), 3.55–3.49 (m, 2H), 1.97–1.92 (m, 2H), 1.79–1.74 (m, 2H). MS (ESI), *m/z*: 510.23 [M + H]⁺.

5-(4-(((1-(5-Nitropyridin-2-yl)piperidin-4-yl)amino)methyl)-benzylidene)pyrimidine-2,4,6-(1H,3H,5H)-trione (12a). Yield: 35.2%. HPLC purity: 98.8%. White solid. ¹H NMR (400 MHz, DMSO-*d*₆): δ 10.01 (s, 2H), 8.97–8.98 (m, 1H), 8.26–8.22 (m, 1H), 7.27 (d, 2H, *J* = 8.0 Hz), 7.08 (d, 2H, *J* = 7.6 Hz), 7.01 (d, 2H, *J* = 6.4 Hz), 5.98 (s, 1H), 4.60–4.57 (m, 2H), 4.38–4.36 (m, 2H), 4.08 (s, 2H), 2.18–2.16 (m, 2H), 1.49–1.47 (m, 2H). MS (ESI), *m/z*: 451.16 [M – H][–].

***N*-(1-(5-Nitropyridin-2-yl)piperidin-4-yl)-*N*-(4-((2,4,6-trioxotetrahydropyrimidin-5(2H)-ylidene)methyl)benzyl)methanesulfonamide (12b).** Yield: 65.4%. HPLC purity: 98.7%. Yellow solid. ¹H NMR (400 MHz, DMSO-*d*₆): δ 11.39 (s, 1H), 11.24 (s, 1H), 8.92–8.91 (m, 1H), 8.25 (s, 1H), 8.16 (dd, 1H, *J* = 9.6 Hz, *J* = 2.8 Hz), 7.44 (d, 2H, *J* = 8.4 Hz), 6.93 (d, 2H, *J* = 9.6 Hz), 4.60 (m, 1H), 4.46 (s, 2H), 4.09–4.03 (m, 2H), 3.09 (s, 3H), 3.04–2.99 (m, 1H), 1.82–1.54 (m, 4H). MS (ESI), *m/z*: 528.15 [M – H][–].

Methyl 3-(*N*-(1-(5-Nitropyridin-2-yl)piperidin-4-yl)-*N*-(4-((2,4,6-trioxotetrahydropyrimidin-5(2H)-ylidene)methyl)benzyl)sulfamoyl)thiophene-2-carboxylate (12c). Yield: 31.3%. HPLC purity: 98.9%. Yellow solid. ¹H NMR (400 MHz, DMSO-*d*₆): δ 9.98 (s, 2H), 8.90 (d, 1H, *J* = 2.8 Hz), 8.12 (dd, 1H, *J* = 9.2 Hz, *J* = 2.8 Hz), 7.90 (d, 1H, *J* = 5.2 Hz), 7.37 (d, 1H, *J* = 5.2 Hz), 7.05 (d, 2H, *J* = 8.0 Hz), 6.91–6.89 (m, 3H), 5.90 (s, 1H), 4.53–4.50 (m, 4H), 3.87 (s, 3H), 2.95–2.93 (m, 2H), 1.54 (s, 4H). MS (ESI), *m/z*: 654.12 [M – H][–].

2-(4-(((4-((2,4,6-Trioxotetrahydropyrimidin-5(2H)-ylidene)methyl)benzyl)amino)piperidin-1-yl)nicotinonitrile (12d). Yield: 40.2%. HPLC purity: 99.1%. Yellow solid. ¹H NMR (400 MHz, DMSO-*d*₆): δ 10.01 (s, 2H), 8.75 (s, 2H), 8.42 (dd, 1H, *J* = 4.8 Hz, *J* = 2.0 Hz), 8.10 (dd, 1H, *J* = 7.6 Hz, *J* = 2.0 Hz), 7.30 (d, 1H, *J* = 8.0 Hz), 7.10 (d, 2H, *J* = 8.0 Hz), 6.97–6.94 (m, 1H), 6.00 (1H), 4.27 (d, 2H, *J* = 13.2 Hz), 4.13 (s, 2H), 3.05 (t, 2H, *J* = 12.0 Hz), 2.19 (d, 2H, *J* = 12.0 Hz), 1.69–1.61 (m, 2H). MS (ESI), *m/z*: 431.17 [M – H][–].

***N*-1-(1-(3-Cyanopyridin-2-yl)piperidin-4-yl)-*N*-4-((2,4,6-trioxotetrahydropyrimidin-5(2*H*)-ylidene)methyl)benzyl)methanesulfonamide (12e).** Yield: 65.4%. HPLC purity: 98.9%. Yellow solid. ¹H NMR (400 MHz, DMSO-*d*₆): δ 11.38 (s, 1H), 11.24 (s, 1H), 8.36–8.35 (m, 1H), 8.26 (s, 1H), 8.13 (d, 1H, *J* = 8.0 Hz), 8.04–8.02 (m, 1H), 7.46 (d, 2H, *J* = 8.0 Hz), 6.89–6.86 (m, 1H), 4.47 (s, 2H), 4.28–4.25 (m, 2H), 4.00–3.94 (m, 1H), 3.08 (s, 3H), 3.05–2.97 (m, 2H), 1.83–1.65 (m, 4H). MS (ESI), *m/z*: 509.15 [M – H][–].

Methyl 3-(*N*-1-(1-(3-Cyanopyridin-2-yl)piperidin-4-yl)-*N*-4-((2,4,6-trioxotetrahydropyrimidin-5(2*H*)-ylidene)methyl)benzyl)sulfamoyl)thiophene-2-carboxylate (12f). Yield: 27.8%. HPLC purity: 97.9%. White solid. ¹H NMR (400 MHz, DMSO-*d*₆): δ 9.99 (s, 2H), 8.34 (m, 1H), 8.25 (s, 1H), 8.00 (dd, 1H, *J* = 7.6 Hz, *J* = 2.0 Hz), 7.89 (d, 1H, *J* = 5.6 Hz), 7.36 (d, 1H, *J* = 5.6 Hz), 7.04 (d, 2H, *J* = 8.0 Hz), 6.89–6.83 (m, 3H), 5.92 (s, 1H), 4.76 (s, 2H), 4.21–4.16 (m, 3H), 3.87 (s, 3H), 2.93 (t, 2H, *J* = 12.0 Hz), 1.65–1.54 (m, 4H). MS (ESI), *m/z*: 635.13 [M – H][–].

5-Chloro-*N*-1-(1-(3-cyanopyridin-2-yl)piperidin-4-yl)-*N*-4-((2,4,6-trioxotetrahydropyrimidin-5(2*H*)-ylidene)methyl)benzyl)thiophene-2-carboxamide (12g). Yield: 26.4%. HPLC purity: 98.9%. White solid. ¹H NMR (400 MHz, DMSO-*d*₆): δ 9.98 (s, 2H), 8.38 (d, 1H, *J* = 4.0 Hz), 8.02 (d, 1H, *J* = 4.0 Hz), 7.08–6.99 (m, 6H), 6.89–6.85 (m, 1H), 5.93 (s, 1H), 4.68 (s, 2H), 4.31–4.28 (m, 3H), 2.99 (t, 2H, *J* = 12.0 Hz), 1.91–1.82 (m, 4H). MS (ESI), *m/z*: 575.12 [M – H][–].

***N*-1-(1-(3-Cyanopyridin-2-yl)piperidin-4-yl)-3-morpholino-*N*-4-((2,4,6-trioxotetrahydropyrimidin-5(2*H*)-ylidene)methyl)benzyl)propane-1-sulfonamide (12h).** Yield: 33.6%. HPLC purity: 99.6%. White solid. ¹H NMR (400 MHz, DMSO-*d*₆): δ 10.02 (s, 2H), 8.37 (s, 1H), 8.03 (d, 1H, *J* = 8.0 Hz), 7.11 (d, 2H, *J* = 8.0 Hz), 6.96 (d, 2H, *J* = 8.0 Hz), 6.87 (m, 1H), 5.94 (s, 1H), 4.31–4.28 (m, 5H), 3.86–3.64 (m, 6H), 3.00 (m, 8H), 1.94–1.79 (m, 6H). MS (ESI), *m/z*: 622.23 [M – H][–].

5-Bromo-*N*-1-(1-(3-cyanopyridin-2-yl)piperidin-4-yl)-*N*-4-((2,4,6-trioxotetrahydropyrimidin-5(2*H*)-ylidene)methyl)benzyl)thiophene-2-carboxamide (12i). Yield: 21.2%. HPLC purity: 98.8%. White solid. ¹H NMR (400 MHz, DMSO-*d*₆): δ 10.01 (s, 2H), 8.38 (s, 1H), 8.03 (s, 1H), 7.18–6.88 (m, 8H), 4.88 (s, 2H), 4.29 (s, 3H), 3.00 (s, 2H), 1.91–1.82 (m, 4H). MS (ESI), *m/z*: 619.07 [M – H][–].

(3*R*,5*R*,7*R*)-*N*-1-(1-(3-Cyanopyridin-2-yl)piperidin-4-yl)-*N*-4-((2,4,6-trioxotetrahydropyrimidin-5(2*H*)-ylidene)methyl)benzyl)adamantane-1-carboxamide (12j). Yield: 39.2%. HPLC purity: 98.8%. White solid. ¹H NMR (400 MHz, DMSO-*d*₆): δ 9.96 (s, 2H), 8.37 (d, 2H, *J* = 4.4 Hz), 8.02 (d, 1H, *J* = 7.2 Hz), 6.90–6.85 (m, 4H), 5.91 (s, 1H), 4.42–4.27 (m, 4H), 1.98–1.54 (m, 12H). MS (ESI), *m/z*: 593.28 [M – H][–].

***N*-1-(1-(3-Cyanopyridin-2-yl)piperidin-4-yl)-*N*-4-((2,4,6-trioxotetrahydropyrimidin-5(2*H*)-ylidene)methyl)benzyl)pentanamide (12k).** Yield: 19.2%. HPLC purity: 98.3%. White solid. ¹H NMR (400 MHz, DMSO-*d*₆): δ 9.98 (s, 2H), 8.37 (d, 2H, *J* = 4.0 Hz), 8.22 (s, 2H), 8.01 (d, 1H, *J* = 8.0 Hz), 6.98–6.86 (m, 4H), 5.93 (s, 1H), 4.44 (s, 2H), 4.41 (s, 1H), 4.26 (d, 2H, *J* = 12.0 Hz), 3.05–2.94 (m, 6H), 2.17 (t, 2H, *J* = 8.0 Hz), 1.71–0.79 (m, 9H). MS (ESI), *m/z*: 515.23 [M – H][–].

1-(1-(3-Cyanopyridin-2-yl)piperidin-4-yl)-3-ethyl-1-(4-((2,4,6-trioxotetrahydropyrimidin-5(2*H*)-ylidene)methyl)benzyl)urea (12l). Yield: 44.2%. HPLC purity: 98.7%. Yellow solid. ¹H NMR (400 MHz, DMSO-*d*₆): δ 11.38 (s, 1H), 11.24 (s, 1H), 8.37–8.36 (m, 1H), 8.25 (s, 1H), 8.12 (d, 2H, *J* = 8.4 Hz), 8.04–8.01 (m, 1H), 7.30 (d, 2H, *J* = 8.4 Hz), 6.89–6.86 (m, 1H), 6.48–6.47 (m, 1H), 4.48 (s, 2H), 4.94 (s, 2H), 4.28–4.25 (m, 3H), 3.13–2.05 (m, 4H), 1.64 (s, 4H), 1.00 (t, 3H, *J* = 6.8 Hz). MS (ESI), *m/z*: 502.21 [M – H][–].

1-(1-(3-Cyanopyridin-2-yl)piperidin-4-yl)-3-methyl-1-(4-((2,4,6-trioxotetrahydropyrimidin-5(2*H*)-ylidene)methyl)benzyl)thiourea (12m). Yield: 34.2%. HPLC purity: 99.6%. Yellow solid. ¹H NMR (400 MHz, DMSO-*d*₆): δ 11.39 (s, 1H), 11.24 (s, 1H), 8.38–8.36 (m, 1H), 8.25 (s, 1H), 8.13 (d, 2H, *J* = 8.4 Hz), 8.04–8.02 (m, 1H), 7.66 (brs, 1H), 7.25 (d, 2H, *J* = 8.4 Hz), 6.94 (m, 1H), 5.18 (brs, 1H), 4.94 (s, 2H), 4.28 (d, 2H, *J* = 12.4 Hz), 3.02 (t, 2H, *J* = 12.4

Hz, *J* = 10.8 Hz), 2.94 (d, 3H, *J* = 4 Hz), 1.74–1.62 (m, 4H). MS (ESI), *m/z*: 503.17 [M – H][–].

***N*-1-(4-(Difluoromethoxy)benzoyl)piperidin-4-yl)-*N*-4-((2,4,6-trioxotetrahydropyrimidin-5(2*H*)-ylidene)methyl)benzyl)methanesulfonamide (12n).** Yield: 20.7%. HPLC purity: 99.1%. Yellow solid. ¹H NMR (400 MHz, DMSO-*d*₆): δ 11.40 (s, 1H), 11.25 (s, 1H), 8.27 (s, 1H), 8.14 (d, 2H, *J* = 8.4 Hz), 7.47 (d, 2H, *J* = 8.0 Hz), 7.21 (d, 2H, *J* = 7.4 Hz), 7.20 (d, 2H, *J* = 8.4 Hz), 7.40 (d, 2H, *J* = 8.0 Hz), 4.51–4.37 (m, 4H), 4.00–3.94 (m, 1H), 3.06 (s, 3H), 1.78–1.61 (m, 4H). MS (ESI), *m/z*: 577.15 [M – H][–].

***N*-1-(3-Fluoro-4-(trifluoromethyl)benzoyl)piperidin-4-yl)-*N*-4-((2,4,6-trioxotetrahydropyrimidin-5(2*H*)-ylidene)methyl)benzyl)methanesulfonamide (12o).** Yield: 18.2%. HPLC purity: 99.5%. Yellow solid. ¹H NMR (400 MHz, DMSO-*d*₆): δ 11.39 (s, 1H), 11.25 (s, 1H), 8.27 (s, 1H), 8.14 (d, 2H, *J* = 8.0 Hz), 7.85 (t, 1H, *J* = 8.0 Hz), 7.58 (d, 2H, *J* = 10.8 Hz), 7.47 (d, 2H, *J* = 8.4 Hz), 7.40 (d, 2H, *J* = 8.0 Hz), 4.52 (m, 4H), 4.01–4.00 (m, 1H), 3.11–2.78 (m, 5H), 1.82–1.62 (m, 4H). MS (ESI), *m/z*: 597.14 [M – H][–].

***N*-1-(3-(1,1,2,2-Tetrafluoroethoxy)benzoyl)piperidin-4-yl)-*N*-4-((2,4,6-trioxotetrahydropyrimidin-5(2*H*)-ylidene)methyl)benzyl)methanesulfonamide (12p).** Yield: 45.4%. HPLC purity: 97.8%. Yellow solid. ¹H NMR (400 MHz, DMSO-*d*₆): δ 11.39 (s, 1H), 11.24 (s, 1H), 8.27 (s, 1H), 8.14 (d, 2H, *J* = 8.4 Hz), 7.54 (t, 1H, *J* = 8.0 Hz), 7.48 (d, 2H, *J* = 8.4 Hz), 7.36–7.34 (m, 2H), 7.27 (s, 1H), 6.81 (t, 1H, *J* = 5.2 Hz), 4.51–4.36 (m, 4H), 3.98 (m, 1H), 3.05 (s, 3H), 1.78–1.62 (m, 4H). MS (ESI), *m/z*: 627.15 [M – H][–].

***N*-1-(4-Nitropyridin-2-yl)piperidin-4-yl)-4-((2,4,6-trioxotetrahydropyrimidin-5(2*H*)-ylidene)methyl)benzamide (14a).** Yield: 35.2%. HPLC purity: 98.6%. Yellow solid. ¹H NMR (400 MHz, DMSO-*d*₆): δ 11.44 (s, 1H), 11.28 (s, 1H), 8.98 (d, 1H, *J* = 2.8 Hz), 8.46 (d, 1H, *J* = 6.8 Hz), 8.29 (s, 1H), 8.22 (dd, 1H, *J* = 9.6 Hz, *J* = 2.8 Hz), 8.05 (d, 2H, *J* = 8.4 Hz), 7.89 (d, 2H, *J* = 8.4 Hz), 7.02 (d, 1H, *J* = 9.6 Hz), 4.53 (d, 2H, *J* = 8.8 Hz), 4.20–4.19 (m, 1H), 3.23 (t, 2H, *J* = 12.0 Hz), 1.97–1.94 (m, 2H), 1.59–1.51 (m, 2H). MS (ESI), *m/z*: 465.14 [M – H][–].

***N*-1-(5-Nitropyridin-2-yl)piperidin-4-yl)-4-((2,4,6-trioxotetrahydropyrimidin-5(2*H*)-ylidene)methyl)benzamide (14b).** Yield: 21.0%. HPLC purity: 99.6%. White solid. ¹H NMR (400 MHz, DMSO-*d*₆): δ 10.12 (s, 2H), 8.98–8.97 (m, 1H), 8.24–8.19 (m, 1H), 8.05 (d, 1H, *J* = 8.4 Hz), 7.87 (d, 1H, *J* = 8.0 Hz), 7.62 (d, 1H, *J* = 8.0 Hz), 7.08 (d, 1H, *J* = 8.0 Hz), 7.03–7.00 (m, 1H), 5.94 (s, 1H), 4.52 (s, 2H), 4.17 (m, 1H), 3.12–3.19 (m, 2H), 1.96–1.91 (m, 2H), 1.56–1.50 (m, 2H). MS (ESI), *m/z*: 465.14 [M – H][–].

***N*-1-(3-Cyanopyridin-2-yl)piperidin-4-yl)-4-((2,4,6-trioxotetrahydropyrimidin-5(2*H*)-ylidene)methyl)benzamide (14c).** Yield: 37.9%. HPLC purity: 99.0%. Yellow solid. ¹H NMR (400 MHz, DMSO-*d*₆): δ 10.06 (s, 2H), 8.41 (s, 2H), 8.17 (d, 2H, *J* = 8.0 Hz), 8.09–8.05 (m, 1H), 7.63 (d, 2H, *J* = 8.0 Hz), 7.07 (d, 2H, *J* = 8.0 Hz), 6.93–6.88 (m, 1H), 5.97 (s, 1H), 4.26–4.23 (m, 4H), 4.09 (m, 1H), 3.19–3.14 (m, 2H), 1.91–1.88 (m, 2H), 1.69–1.64 (m, 2H). MS (ESI), *m/z*: 445.15 [M – H][–].

5-(4-(4-((4-Nitropyridin-2-yl)amino)piperidine-1-carbonyl)benzylidene)pyrimidine-2,4,6(1*H*,3*H*,5*H*)-trione (17a). Yield: 22.8%. HPLC purity: 99.1%. White solid. ¹H NMR (400 MHz, DMSO-*d*₆): δ 10.09 (s, 2H), 7.96–7.94 (m, 1H), 7.61 (d, 2H, *J* = 8.4 Hz), 7.07 (d, 2H, *J* = 8.4 Hz), 7.63–7.89 (m, 3H), 5.95 (s, 1H), 4.10–4.08 (m, 1H), 4.02–3.98 (m, 2H), 1.88–1.82 (m, 2H), 1.53 (t, 2H, *J* = 10.0 Hz). MS (ESI), *m/z*: 465.14 [M – H][–].

5-(4-(4-((5-Nitropyridin-2-yl)amino)piperidine-1-carbonyl)benzylidene)pyrimidine-2,4,6(1*H*,3*H*,5*H*)-trione (17b). Yield: 27.5%. HPLC purity: 98.3%. White solid. ¹H NMR (400 MHz, DMSO-*d*₆): δ 10.09 (s, 2H), 7.96–7.94 (m, 1H), 7.61 (d, 2H, *J* = 8.4 Hz), 7.07 (d, 2H, *J* = 8.4 Hz), 7.63–7.89 (m, 3H), 5.95 (s, 1H), 4.10–4.08 (m, 1H), 4.02–3.98 (m, 2H), 1.88–1.82 (m, 2H), 1.53 (t, 2H, *J* = 10.0 Hz). MS (ESI), *m/z*: 465.14 [M – H][–].

Glucose Consumption/MTT in HepG2 Cell Lines. The HepG2 cells (ATCC, Rockville, MD) were grown in DMEM (22.2 mM glucose) containing 10% fetal bovine serum. Two days before the experiment, the cells were plated into 96-well tissue culture plates and treated with 0.1 μM insulin. When the cells reached confluence, the medium was removed and the DMEM (22.2 mM glucose) containing

these compounds (10 μM), metformin (1.0 mM), and rosiglitazone (10 μM , Sigma-Aldrich, St. Louis, MO) were added to all wells. After 24 h, the culture medium was sampled and its glucose concentrations were determined by the glucose oxidase method (GENMED SCIENTIFICS, U.S.). The amount of glucose consumption (GC) was calculated by the glucose concentration of blank wells minus the remaining glucose in cell plated wells and divided by corresponding MTT values. The results were recorded from three independent experiments.

Expression of Adiponectin and Leptin in 3T3-L1 Adipocytes. Murine 3T3-L1 preadipocytes (ATCC, Rockville, MD) were plated and grown to 2 days after confluence in six-well culture plates in DMEM containing 10% fetal bovine serum. Preadipocytes were induced to differentiate by replacing the medium with serum-containing DMEM containing 0.5 mM methyl-3-isobutylxanthine (IBMX), 0.25 μM dexamethasone (DEX), and 1 $\mu\text{g}/\text{mL}$ insulin. Two days later, the medium was again changed to serum-containing DMEM that contained insulin but no IBMX or DEX. Two days later, the medium was again changed to the original DMEM containing 10% fetal bovine serum in the absence of any differentiating reagents and was replaced every two days. Full differentiation is usually achieved by 8–12 days. The twelfth day after differentiation, the culture medium was replaced by DMEM supplemented with compounds (10 μM), rosiglitazone (10 μM), and metformin (1.0 mM). After 24 h, the determination of adiponectin and leptin was performed by commercial ELISA kits (BOSTER, Wuhan, China). The results were recorded for three independent experiments.

Animal Model and Treatment of NAFLD. Male Wistar rats (160–180g) were purchased from Western China Experimental Animal Center (Chengdu, China). Every five rats were placed in one cage on a 12 h day/night cycle and quarantined for 1 week. All animals, which were maintained under controlled conditions and had free access to standard laboratory chow and water, received human care according to National Institutes of Health Guidelines before and during experiment. After acclimatization for 1 week, animals were assigned to five groups randomly consisting of 10 rats each (G1–G5). In this study, G1–G4 groups were given access to high fat diet and G5 group was given access to normal diet throughout the experimental period. The high fat diet was purchased from Shuangshi Experimental Animal Diet Centre (Nanjing, China), which consisted of 20% lard stearin (w/w) and 10% sucrose, and 0.1% bile salt was added into normal diet. The rats received a normal diet with 18.94% of energy derived from fat, 31.67% from protein, and 49.39% from carbohydrates and received a high fat diet with 50.55% of energy derived from fat, 15.72% from protein, and 33.73% from carbohydrates. In addition to the daily high fat diet, metformin (150 $\text{mg kg}^{-1} \text{ day}^{-1}$), 7h (25 $\text{mg kg}^{-1} \text{ day}^{-1}$), and 7q (25 $\text{mg kg}^{-1} \text{ day}^{-1}$) suspended in Tween 80 and 5% saline were orally administered correspondingly to the G1–G3 group, respectively. After the experimental period was completed, all rats were anesthetized and samples were collected. Meanwhile, body, liver, and fat weight of rats were recorded. Serum levels of triglycerides, LDL-c, HDL-c, AST, ALT, and glucose were measured using a multifunctional biochemistry analyzer Olympus AU2700 (Olympus, Tokyo, Japan). The fasting insulin was tested by commercial kits (R&D Systems, Minneapolis, MN, U.S.). The serum levels of adiponectin and leptin were determined by commercial ELISA kits (BOSTER, Wuhan, China). The percentages were calculated using $[(V_{\text{HFD}} - V_{\text{treatment}})/V_{\text{HFD}}] \times 100$. Liver tissues were homogenized in 50 mM Tris-HCl buffer (pH 7.4), containing 150 mM NaCl, 1 mM phenylmethylsulfonyl fluoride, and 1 mM EDTA. The liver content of triglycerides and total cholesterol were analyzed using a diagnostic kit (Jiancheng, Nanjing, China) according to the manufacturer's instruction. Liver and adipose samples were fixed in 4% buffered formalin and embedded in Tissue-Tek OCT compound (Sakura Finetek USA, U.S.) and paraffin for H&E staining.

Pharmacokinetics of 7h in Sprague–Dawley Rats. Two groups ($n = 5$) of male and female Sprague–Dawley rats (180–200g) were fasted overnight and received 7h as an intravenous (iv) dose (10 mg/kg) or by oral gavage (50 mg/kg , dissolved in Tween 80). Blood samples (0.5 mL) were obtained from retro-orbital

bleeding at 0.05, 0.25, 0.5, 1, 3, 6, 8, and 24 h postdose for the iv group and at 0.25, 0.5, 1, 3, 6, 8, and 24 h postdose for the po group. At each time point, three mice were bled resulting in a composite pharmacokinetic profile. The tubes were inverted several times to ensure mixing and placed on ice. Plasma was obtained following centrifugation at 4 $^{\circ}\text{C}$ (1500–2000g). Plasma samples were stored at -20°C until analysis by a UPLC system.

Animal Model and Treatment of Diet-Induced Obesity. C57BL/6J mice were obtained from Western China Experimental Animal Center and housed individually in a room maintained at 25 $^{\circ}\text{C}$ on a light/dark schedule. For DIO mice, 3-week-old male C57BL/6J mice were fed a high fat diet (HFD, Research Diets) ad libitum for 8 weeks. Then these animals were assigned to four groups randomly consisting of 10 mice each. The rats received a normal diet with 18.94% of energy derived from fat, 31.67% from protein, and 49.39% from carbohydrates and received a high fat diet with 60.0% of calories from fat, 20.0% from protein, and 20.0% from carbohydrates. HFD + Met (150 $\text{mg kg}^{-1} \text{ day}^{-1}$) and HFD + 7h (25 $\text{mg kg}^{-1} \text{ day}^{-1}$) in PEG₄₀₀ or vehicle were orally administered per day for 7 weeks. Body weight and food intake were measured per day. After all animals were sacrificed, and serum levels of markers were analyzed according to the NAFLD procedure. The percentages were calculated using $[(V_{\text{HFD}} - V_{\text{treatment}})/V_{\text{HFD}}] \times 100$. Oral glucose tolerance test (OGTT) and intravenous glucose tolerance test (IGTT) were performed in 7h-treated DIO mice ($n = 5$) for 6 weeks after 1 night of fasting. Blood were sampled from the tail vein of mice at 0, 15, 30, 60, 90, 120, and 180 min after an oral glucose load of 3.0 g/kg or intravenous glucose load of 0.5 g/kg of body weight.

■ ASSOCIATED CONTENT

● Supporting Information

Synthesis and analytical data of all intermediates not described in the Experimental Section; biological studies and details of PK study in SD rats, and HPLC chromatograms of representative compounds. This material is available free of charge via the Internet at <http://pubs.acs.org>.

■ AUTHOR INFORMATION

Corresponding Author

*Phone: +86-28-85164063. E-mail: lijuan17@hotmail.com.

Author Contributions

[†]These authors contributed equally.

Notes

The authors declare no competing financial interest.

■ ACKNOWLEDGMENTS

We are grateful to the National Key Programs of China during the 12th Five-Year Plan Period (Grant 2012ZX09103101-033).

■ ABBREVIATIONS USED

NAFLD, nonalcoholic fatty liver disease; NASH, nonalcoholic steatohepatitis; HCC, hepatocellular carcinoma; GC, glucose consumption; TsCl, *p*-toluenesulfonyl chloride; EDCl, 1-(3-dimethylaminopropyl)-3-ethylcarbodiimide hydrochloride; NaBH₄, sodium borohydride; DMF, dimethylformamide; TZD, thiazolidinedione; H&E, hematoxylin and eosin; HFD, high fat diet; MTT, 3-(4,5-dimethylthiazol-2-yl)-2,5-diphenyl-tetrazolium bromide; LDL-c, low-density lipoprotein cholesterol; HDL-c, high-density lipoprotein cholesterol; FFA, free fatty acid; ALT, alanine transaminase; AST, aspartate aminotransferase; DIO, diet-induced obesity; OGTT, oral glucose tolerance test; IGTT, intravenous glucose tolerance test

■ REFERENCES

- (1) Angulo, P. Nonalcoholic fatty liver disease. *N. Engl. J. Med.* **2002**, *346*, 1221–1231.
- (2) Polyzos, S. A.; Kountouras, J.; Zavos, C.; Tsiaousi, E. The role of adiponectin in the pathogenesis and treatment of non-alcoholic fatty liver disease. *Diabetes Obes. Metab.* **2010**, *12*, 365–383.
- (3) Adams, L. A.; Angulo, P. Treatment of non-alcoholic fatty liver disease. *Postgrad. Med. J.* **2006**, *82*, 315–322.
- (4) Day, C. P. Non-alcoholic fatty liver disease: current concepts and management strategies. *Clin. Med.* **2006**, *6*, 19–25.
- (5) Hübscher, S. G. Histological assessment of non-alcoholic fatty liver disease. *Histopathology* **2006**, *49*, 450–465.
- (6) Parekh, S.; Anania, F. A. Abnormal lipid and glucose metabolism in obesity: implications for nonalcoholic fatty liver disease. *Gastroenterology* **2007**, *132*, 2191–2207.
- (7) Dixon, J. B.; Bhathal, P. S.; O'Brien, P. E. Nonalcoholic fatty liver disease: predictors of nonalcoholic steatohepatitis and liver fibrosis in the severely obese. *Gastroenterology* **2001**, *121*, 91–100.
- (8) Nugent, C.; Younossi, Z. M. Evaluation and management of obesity-related nonalcoholic fatty liver disease. *Nat. Clin. Pract. Gastroenterol. Hepatol.* **2007**, *4*, 432–441.
- (9) Berg, A. H.; Combs, T. P.; Scherer, P. E. ACRP30/adiponectin: an adipokine regulating glucose and lipid metabolism. *Trends Endocrinol. Metab.* **2002**, *13*, 84–89.
- (10) Christos, S.; Mantzoros, M. D. The role of leptin in human obesity and disease: a review of current evidence. *Ann. Intern. Med.* **1999**, *130*, 671–680.
- (11) Nedvidkova, J.; Smitka, K.; Kopsky, V.; Hainer, V. Adiponectin, an adipocyte-derived protein. *Physiol. Res.* **2005**, *54*, 133–140.
- (12) Xu, A.; Wang, Y.; Keshaw, H.; Xu, L. Y.; Lam, K. S.; Cooper, G. J. The fat-derived hormone adiponectin alleviates alcoholic and nonalcoholic fatty liver diseases in mice. *J. Clin. Invest.* **2003**, *112*, 91–100.
- (13) Whitehead, J. P.; Richards, A. A.; Hickman, I. J.; Macdonald, G. A.; Prins, J. B. Adiponectin, a key adipokine in the metabolic syndrome. *Diabetes Obes. Metab.* **2006**, *8*, 264–280.
- (14) Hotta, K.; Funahashi, T.; Arita, Y.; Takahashi, M.; Matsuda, M.; Okamoto, Y.; Iwahashi, H.; Kuriyama, H.; Ouchi, N.; Sakai, N.; Nakajima, T.; Hasegawa, K.; Matsuzawa, Y. Plasma concentrations of a novel, adipose-specific protein, adiponectin, in type 2 diabetic patients. *Arterioscler., Thromb., Vasc. Biol.* **2000**, *15*, 1595–1599.
- (15) Valerio, N.; Melania, M.; Paolo, C.; Vincenzo, D.; Rita, D.; Fiorella, P.; Donatella, C.; Roberto, G.; Matilde, M. Leptin, free leptin index, insulin resistance and liver fibrosis in children with non-alcoholic fatty liver disease. *Eur. J. Endocrinol.* **2006**, *155*, 735–743.
- (16) Saltiel, A. R.; Kahn, C. R. Insulin signalling and the regulation of glucose and lipid metabolism. *Nature* **2001**, *414*, 799–806.
- (17) Ma, L.; Li, S. L.; Zheng, H.; Chen, J. Y.; Lin, L.; Ye, X.; Chen, Z. Z.; Xu, Q. Y.; Chen, T.; Yang, J. C.; Qiu, N.; Wang, G. C.; Peng, A. H.; Ding, Y.; Wei, Y.-Q.; Chen, L. J. Synthesis and biological activity of novel barbituric and thiobarbituric acid derivatives against non-alcoholic fatty liver disease. *Eur. J. Med. Chem.* **2011**, *46*, 2003–2010.
- (18) Zheng, H.; Li, S. L.; Ma, L.; Cheng, L.; Deng, C. Y.; Chen, Z. Z.; Xie, C. F.; Xiang, M. L.; Jiang, W.; Chen, L. J. A novel agonist of PPAR- γ based on barbituric acid alleviates the development of non-alcoholic fatty liver disease by regulating adipocytokine expression and preventing insulin resistance. *Eur. J. Pharmacol.* **2011**, *659*, 244–251.
- (19) Ma, L.; Chen, J. Y.; Liang, X. L.; Xie, C. F.; Deng, C. Y.; Huang, L.; Peng, A. H.; Wei, Y.-Q.; Chen, L. J. Synthesis and evaluation of 5-benzylidene-thiazolidine-2,4-dione derivatives for the treatment of non-alcoholic fatty liver disease. *Arch. Pharm. (Weinheim, Ger.)* **2012**, *345*, 517–524.
- (20) Vincent, P.; Jasna, K.; David, C.; Dennis, D. C.; Jeffrey, P. S.; Karen, R.; Fabienne, B. C.; Delphine, V.; Montserrat, C.; Christian, C.; Corinne, G.; Bernard, F.; Dominique, P.; Didier, L.; Denise, G.; Anthony, N.; Pierre, A. V.; Susanna, C.; Christian, R.; Thomas, R. Furan-2-ylmethylene thiazolidinediones as novel, potent, and selective inhibitors of phosphoinositide 3-kinase γ . *J. Med. Chem.* **2006**, *49*, 3857–3871.
- (21) Qin, N.; Li, C. B.; Jin, M. N.; Shi, L. H.; Duan, H. Q.; Niu, W. Y. Synthesis and biological activity of novel tiliroside derivants. *Eur. J. Med. Chem.* **2011**, *46*, 5189–5195.
- (22) Mosmann, T. Rapid colorimetric assay for cellular growth and survival: application to proliferation and cytotoxicity assays. *J. Immunol. Methods* **1983**, *65*, 55–63.
- (23) Sophie, P.; Peter, R. M.; Steve, S.; Veronique, G. Fluorine in medicinal chemistry. *Chem. Soc. Rev.* **2008**, *37*, 320–330.